ISSN 1948-0210 (online)

# World Journal of *Stem Cells*

*World J Stem Cells* 2018 December 26; 10(12): 183-227

Published by Baishideng Publishing Group Inc

WJSC World Journal of Stem Cells

Contents

Monthly Volume 10 Number 12 December 26, 2018

## MINIREVIEWS

183 Cancer stem cell impact on clinical oncology

*Toledo-Guzmán ME, Bigoni-Ordóñez GD, Ibáñez Hernández M, Ortiz-Sánchez E*

## ORIGINAL ARTICLE

### Basic Study

196 Functional and molecular mechanism of intracellular pH regulation in human inducible pluripotent stem cells

*Chao SC, Wu GJ, Huang SF, Dai NT, Huang HK, Chou MF, Tsai YT, Lee SP, Loh SH*

196 Platelet-rich plasma enhances adipose-derived stem cell-mediated angiogenesis in a mouse ischemic hindlimb model

*Chen CF, Liao HT*

**ABOUT COVER**

Editorial Board Member of *World Journal of Stem Cells*, Nils O Schmidt, MD, Associate Professor, Department of Neurosurgery, University Medical Center Hamburg-Eppendorf, Hamburg 20246, Germany

**AIM AND SCOPE**

*World Journal of Stem Cells* (*World J Stem Cells*, *WJSC*, online ISSN 1948-0210, DOI: 10.4252), is a peer-reviewed open access academic journal that aims to guide clinical practice and improve diagnostic and therapeutic skills of clinicians.

*WJSC* covers topics concerning all aspects of stem cells: embryonic, neural, hematopoietic, mesenchymal, tissue-specific, and cancer stem cells; the stem cell niche, stem cell genomics and proteomics, and stem cell techniques and their application in clinical trials.

We encourage authors to submit their manuscripts to *WJSC*. We will give priority to manuscripts that are supported by major national and international foundations and those that are of great basic and clinical significance.

**INDEXING/ABSTRACTING**

*World Journal of Stem Cells (WJSC)* is now indexed in PubMed, PubMed Central, Science Citation Index Expanded (also known as SciSearch®), Journal Citation Reports/Science Edition, Biological Abstracts, and BIOSIS Previews. The 2018 Edition of Journal Citation Reports cites the 2017 impact factor for *WJSC* as 4.376 (5-year impact factor: N/A), ranking *WJSC* as 7 among 24 journals in Cell and Tissue Engineering (quartile in category Q2), and 65 among 190 journals in Cell Biology (quartile in category Q2).



NAME OF JOURNAL
*World Journal of Stem Cells*

ISSN
ISSN 1948-0210 (online)

LAUNCH DATE
December 31, 2009

FREQUENCY
Monthly



Baishideng Publishing Group Inc
7901 Stoneridge Drive, Suite 501, Pleasanton, CA 94588, USA
Telephone: +1-925-2238242
Fax: +1-925-2238243
E-mail: editorialoffice@wjgnet.com
Help Desk: https://www.f6publishing.com/helpdesk
https://www.wjgnet.com

PUBLISHER
Baishideng Publishing Group Inc
7901 Stoneridge Drive, Suite 501,
Pleasanton, CA 94588, USA
Telephone: +1-925-2238242
Fax: +1-925-2238243
E-mail: bpgoffice@wjgnet.com
Help Desk: https://www.f6publishing.com/helpdesk
https://www.wjgnet.com

PUBLICATION DATE
December 26, 2018



INSTRUCTIONS TO AUTHORS
https://www.wjgnet.com/bpg/gerinfo/204

ONLINE SUBMISSION
https://www.f6publishing.com

World Journal of Stem Cells

Submit a Manuscript: https://www.f6publishing.com

*World J Stem Cells* 2018 December 26; 10(12): 196-211

DOI: 10.4252/wjsc.v10.i12.196

ISSN 1948-0210 (online)

ORIGINAL ARTICLE

Basic Study

# Functional and molecular mechanism of intracellular pH regulation in human inducible pluripotent stem cells

Shih-Chi Chao, Gwo-Jang Wu, Shu-Fu Huang, Niann-Tzyy Dai, Hsu-Kai Huang, Mei-Fang Chou, Yi-Ting Tsai, Shiao-Pieng Lee, Shih-Hurng Loh

Shih-Chi Chao, Shih-Hurng Loh, Graduate Institute of Life Sciences, National Defense Medical Center, Taipei 11490, Taiwan

Gwo-Jang Wu, Department of Obstetrics and Gynecology, Tri-Service General Hospital, National Defense Medical Center, Taipei 11490, Taiwan

Shu-Fu Huang, Mei-Fang Chou, Shih-Hurng Loh, Department of Pharmacy Practice, Tri-Service General Hospital, National Defense Medical Center, Taipei 11490, Taiwan

Niann-Tzyy Dai, Division of Plastic and Reconstructive Surgery, Department of Surgery, Tri-Service General Hospital, National Defense Medical Center, Taipei 11490, Taiwan

Hsu-Kai Huang, Division of Chest Surgery, Department of Surgery, Tri-Service General Hospital, National Defense Medical Center, Taipei 11490, Taiwan

Yi-Ting Tsai, Graduate Institute of Medical Sciences, National Defense Medical Center, Taipei 11490, Taiwan

Yi-Ting Tsai, Division of Cardiovascular Surgery, Department of Surgery, Tri-Service General Hospital, National Defense Medical Center, Taipei 11490, Taiwan

Shiao-Pieng Lee, Division of Oral and Maxillofacial Surgery, Department of Dentistry, School of Dentistry, Tri-Service General Hospital and National Defense Medical Center, Taipei 11490, Taiwan

Shih-Hurng Loh, Department of Pharmacology, National Defense Medical Center, Taipei 11490, Taiwan

ORCID number: Shih-Chi Chao (0000-0002-0920-9340); Gwo-Jang Wu (0000-0001-5360-8018); Shu-Fu Huang (0000-0002-4593-1779); Niann-Tzyy Dai (0000-0003-2066-574X); Hsu-Kai Huang (0000-0002-4358-4822); Mei-Fang Chou (0000-0001-5515-593X); Yi-Ting Tsai (0000-0001-9439-9734); Shiao-Pieng Lee (0000-0002-7345-2062); Shih-Hurng Loh (0000-0001-9269-5580).

Author contributions: Chao SC and Loh SH performed the majority of experiments and analyzed the data; Chao SC, Wu GJ, Dai NT and Loh SH performed conception and design; Wu GJ, Dai NT and Loh SH participated equally in iPSC treatment and providing; Chao SC, Wu GJ, Huang SF, Dai NT, Huang SK, Tsai YT, Lee SP and Loh SH coordinated and interpreted the research; Cha SC and Loh SH wrote the paper; Cha SC, Wu GJ, Huang SF and Loh SH drafted the article or making critical revisions related to important intellectual content of the manuscript; Loh SH final approval of the version of the article to be published.

Supported by Ministry of Science and Technology Grants of Taiwan, No. MOST 106-2320-B-016-003-MY2 (to Loh SH) and No. MOST 106-2314-B-016-037-MY3 (to Tsai YT); National Defense Medical Center Grants of Taiwan, No. MAB-106-033 (to Loh SH), No. MAB-105-043 and No. MAB-106-034 (to Dai NZ); Teh-Tzer Study Group for Human Medical Research Foundation of Taiwan, No. A1061037 and No. A1061054 (to Loh SH).

Institutional review board statement: The manuscript is approved by Institutional Review Board of Tri-Service General Hospital.

Conflict-of-interest statement: All authors declare no potential conflict of interest.



Manuscript source: Invited manuscript

Corresponding author to: Shih-Hurng Loh, DPhil, Director, Full Professor, Department of Pharmacology, and Department of Pharmacy Practice, Tri-Service General Hospital, National

Defense Medical Center, No. 161, Sec. 6, Minquan E. Rd., Taipei 11490, Taiwan. shloh@ndmctsgh.edu.tw
Telephone: +886-2-87924861
Fax: +886-2-87924861

Received: October 17, 2018
Peer-review started: October 17, 2018
First decision: October 26, 2018
Revised: November 14, 2018
Accepted: December 4, 2018
Article in press: December 5, 2018
Published online: December 26, 2018

## Abstract

***AIM***

To establish a functional and molecular model of the intracellular pH ($pH_i$) regulatory mechanism in human induced pluripotent stem cells (hiPSCs).

***METHODS***

hiPSCs (HPS0077) were kindly provided by Dr. Dai from the Tri-Service General Hospital (IRB No. B-106-09). Changes in the $pH_i$ were detected either by microspectrofluorimetry or by a multimode reader with a pH-sensitive fluorescent probe, BCECF, and the fluorescent ratio was calibrated by the high $K^+$/nigericin method. $NH_4Cl$ and Na-acetate prepulse techniques were used to induce rapid intracellular acidosis and alkalization, respectively. The buffering power ($\beta$) was calculated from the $\Delta pH_i$ induced by perfusing different concentrations of $(NH_4)_2SO_4$. Western blot techniques and immunocytochemistry staining were used to detect the protein expression of $pH_i$ regulators and pluripotency markers.

***RESULTS***

In this study, our results indicated that (1) the steady-state $pH_i$ value was found to be 7.5 ± 0.01 ($n$ = 20) and 7.68 ± 0.01 ($n$ =20) in HEPES and 5% $CO_2/HCO_3^-$-buffered systems, respectively, which were much greater than that in normal adult cells (7.2); (2) in a $CO_2/HCO_3^-$-buffered system, the values of total intracellular buffering power ($\beta$) can be described by the following equation: $\beta_{tot}$ = 107.79 $(pH_i)^2$ - 1522.2 ($pH_i$) + 5396.9 (correlation coefficient $R^2$ = 0.85), in the estimated $pH_i$ range of 7.1-8.0; (3) the $Na^+/H^+$ exchanger (NHE) and the $Na^+/HCO_3^-$ cotransporter (NBC) were found to be functionally activated for acid extrusion for $pH_i$ values less than 7.5 and 7.68, respectively; (4) V-ATPase and some other unknown $Na^+$-independent acid extruder(s) could only be functionally detected for $pH_i$ values less than 7.1; (5) the $Cl^-$/ $OH^-$ exchanger (CHE) and the $Cl^-/HCO_3^-$ anion exchanger (AE) were found to be responsible for the weakening of intracellular proton loading; (6) besides the CHE and the AE, a $Cl^-$-independent acid loading mechanism was functionally identified; and (7) in hiPSCs, a strong positive correlation was observed between the loss of pluripotency and the weakening of the intracellular acid extrusion mechanism, which included a decrease in the steady-state $pH_i$ value and diminished the functional activity and protein expression of the NHE and the NBC.

***CONCLUSION***

For the first time, we established a functional and molecular model of a $pH_i$ regulatory mechanism and demonstrated its strong positive correlation with hiPSC pluripotency.

**Key words:** Microspectrofluorimetry; Human induced pluripotent stem cells; $Na^+/H^+$ exchanger; $Na^+/HCO_3^-$ cotransporter; $Cl^-/OH^-$ exchanger; $Cl^-/HCO_3^-$ exchanger; V-ATPase; Intracellular buffering power; Intracellular pH; BCECF



**Core tip:** For the first time, we established a model of the intracellular pH ($pH_i$) regulation mechanism in human induced pluripotent stem cells (hiPSCs). The steady-state $pH_i$ value of hiPSCs was 7.50-7.68, which greater than that of normal adult cells. The $Na^+$-$H^+$ exchanger, the $Na^+$-$HCO_3^-$ cotransporter and vacuolar-ATPase were the main acid extruders, while the $Cl^-$-$HCO_3^-$ anion exchanger and the $Cl^-$-$OH^-$ exchanger were the main acid loaders. Moreover, the $pH_i$ and acid-extruding mechanism were decreased during the loss of pluripotency in hiPSCs. $pH_i$ regulators represent an attractive target for differentiation efficiency or culture quality.

Chao SC, Wu GJ, Huang SF, Dai NT, Huang HK, Chou MF, Tsai YT, Lee SP, Loh SH. Functional and molecular mechanism of intracellular pH regulation in human inducible pluripotent stem cells. *World J Stem Cells* 2018; 10(12): 196-211
URL: https://www.wjgnet.com/1948-0210/full/v10/i12/196.htm
DOI: https://dx.doi.org/10.4252/wjsc.v10.i12.196

## INTRODUCTION

The homeostasis of intracellular pH ($pH_i$) affects many cellular functions, including cell proliferation, apoptosis, differentiation and epigenetic characteristics[1-7]. The $pH_i$ in mammalian cells is maintained within an optimal narrow range through the combined operation of transmembrane transporters and the intracellular buffering capacity. Thus far, $pH_i$ control in mammalian cells has been divided into the following categories: (1) intracellular buffering; (2) acid extrusion systems; (3) acid loading systems; and (4) monocarboxylate-$H^+$ transport[7-11]. Intracellular buffering power ($\beta$) minimizes immediate changes in $pH_i$, either in an acidic or alkaline direction. The total intracellular buffering power ($\beta_{tot}$) has two components as follows: the intrinsic buffering power

of the cell ($\beta_i$) caused by physicochemical buffers, such as weak acid/base moieties of cytoplasmic proteins, and the buffering capacity caused by intracellular $CO_2/HCO_3^-$ ($\beta_{CO2}$)[10]. Furthermore, different ion transporters are involved in the active $pH_i$ regulatory mechanism. Acid-equivalent extruders, the $Na^+$-$H^+$ exchanger (NHE), the $Na^+$-$HCO_3^-$ cotransporter (NBC) and vacuolar-ATPase (V-ATPase) are the main active acid extruders that are activated against intracellular acidification[7-9,12,13]. In contrast, the acid-equivalent loaders, such as the $Cl^-$-$HCO_3^-$ anion exchanger (AE) and the $Cl^-$-$OH^-$ exchanger (CHE), are activated to prevent intracellular alkalization[12,14,15]. In addition to acid extruders and acid loaders, there is also an $H^+$-monocarboxylate transporter (MCT), which is very important for all mammalian cells because the metabolism and transport of lactate is essential for metabolism and function under physiological or pathological conditions, such as in tumors or hypoxic conditions. The MCT has been demonstrated to play a role either as an acid extruder or an acid loader, depending on the concentration gradient of monocarboxylates, such as lactate acid and pyruvate, between the intracellular and extracellular environments[16,17]. The MCT carrier is stereoselective for L-lactate over D-lactate and has a stoichiometry of 1 $H^+$ with 1 lactate$^-$ anion[18,19].

Recently, the dysregulation of $pH_i$ has been found to be a commonly adaptive feature in different types of cancer cells[20]. In normally differentiated adult cells, the $pH_i$ and extracellular pH ($pH_e$) are generally approximately 7.2 and 7.4, respectively[8,9,13,21]. However, a reversed pH gradient of $pH_i \geqslant 7.2$ and $pH_e \leqslant 7.1$ has been demonstrated in cancer cells. This reversed pH gradient is caused the overexpression and increased set-point of the acid extrusion mechanism[12,20-23]. This dysregulated $pH_i$ feature further promotes tumor progression, invasion and metastasis[21,24-26]. Indeed, metabolic changes have been reported to be a substantial hallmark of cancer cells[27]. Both in the absence or presence of oxygen, cancer cells tend to shift their metabolism from aerobic phosphorylation to aerobic glycolysis, which is known as the Warburg effect. However, the glycolytic byproducts lactate and $H^+$ increase during aerobic glycolysis. Therefore, intracellular acid extruders, such as NHE and MCT, are activated to maintain $pH_i$ homeostasis. The overactivation and/or overexpression of the acid extrusion mechanism results in an increased $pH_i$ that further promotes proliferation and prevents apoptosis in cancer cells[24,26,28,29]. Furthermore, accompanying extracellular acidification causes restructuring of the extracellular matrix and further promotes malicious metastasis and invasion[26,30,31].

Human induced pluripotent stem cells (hiPSCs), which are reprogrammed from somatic cells by expressing pluripotent transcription factors, are defined by their ability for self-renewal and differentiation into the three germ layers[32]. Pluripotent stem cells (PSCs) shared many similar properties with cancer cells, such as increased glycolysis, proliferation and adaptation to hypoxia[33-35]. Therefore, it has been proposed that the $pH_i$ regulatory mechanism in hiPSCs is not typical compared to that in most adult cells. Indeed, a few studies have indicated that changes in $pH_i$ affect the fate of stem cell differentiation. Decreased $pH_i$, either by a deficiency or the inhibition of NHE1, has been found to disturb retinoic acid-induced neuronal differentiation in mouse embryonal carcinoma cells. A similar phenomenon has been claimed to contribute to osteogenesis in human umbilical cord-derived mesenchymal stem cells[1,36]. Furthermore, overexpressed NHE1 has been shown to increase cardiomyocyte differentiation in mouse embryonic stem cells (mESCs)[6]. A recent study has reported that a decreased $pH_i$ by knocking out or inhibiting NHE obstructed drosophila follicle stem cell differentiation and delayed the loss of pluripotency during spontaneous differentiation induced by the removal of LIF/2i[6]. Therefore, an elevated $pH_i$ is considered necessary for PSCs to differentiate. Furthermore, another study has shown that acidic culture medium, caused by the accumulation of lactic acid from glycolysis, promotes pluripotency in both mESCs and hESCs through several mechanisms. However, studies that have optimized the culture environment showed that although acidic culture medium (pH < 7.0) promotes the retention of OCT-4 and pluripotency, it also causes significant growth arrest and an apoptotic effect in mESCs[37]. Notably, although decreasing $pH_i$ has been shown to retain pluripotency during differentiation, the resting $pH_i$ level in the pluripotent state is maintained at $pH_i$ about 7.4 and is greater than that in differentiated adult cells[6]. Therefore, these recent results implicate that PSCs might share a cancer-like $pH_i$ regulatory mechanism and consequently create a reversed pH gradient to promote pluripotent properties. However, there is a lack of reports on the correlation between the $pH_i$ regulatory mechanism and pluripotency in hiPSCs.

Because of the importance of $pH_i$ regulation in hiPSCs, the aims of this study are to further investigate the underlying mechanisms of $pH_i$ regulation in hiPSCs. To determine transporter-mediated membrane fluxes of acid equivalents from measurements of $pH_i$, an accurate knowledge of intracellular buffering power is essential. Therefore, the first aim of this study is to estimate $\beta_i$ and $\beta_{CO2}$, and the second aim is to characterize the active $pH_i$ regulators in hiPSCs to provide the molecular and functional targets of $pH_i$ regulators for future applications in clinics. Finally, the correlation between the $pH_i$ regulatory mechanism and hiPSC pluripotency was examined in this study.

## MATERIALS AND METHODS

### *Cell culture*

The hiPSCs (HPS0077) were a kind gift from Dr. N.Z. Dai (TSGH-IRB No: 100-05-251) from the Tri-Service General Hospital, Taipei, Taiwan. In this study, vitronectin was used to support the growth and adhesion of HPS0077 cells. To prepare the vitronectin-coated culture

plate, 100 μL vitronectin (500 μg/mL) was directly added and mixed into cold DPBS. The vitronectin-DPBS solution was then added into the culture plate at a final concentration of 0.5 μg/cm$^2$ and incubated at room temperature for at least 2 h. This vitronectin-coated culture plate could be used immediately or stored at 4 ℃ for later use within 2 wk. To maintain pluripotency, HPS0077 cells were continuously cultured with mTeSR1 or mTeSR-E8 medium. When the cell colonies were grown to a sufficient size, Accutase was added to the cells at 37 ℃ for 3 min to suspend the cells. The cell suspension was centrifuged at 1000 rpm for 3 min, and the collected cell pellet was resuspended in fresh medium. The vitronectin solution was aspirated, and the cells were seeded in a suitable ratio with mTeSR1 or mTeSR-E8 medium containing 10 μmol/L Y-27632. The Y-27632-containing culture medium was replaced with Y-27632-free medium after 24 h, and the medium was subsequently changed every day. To induce the loss of pluripotency, the mTeSR1 or mTeSR-E8 medium was replaced by mTeSR-E6 medium for 1 to 4 d, and the medium was changed once every two days.

### *Immunocytochemistry staining and immunoblotting*

For immunocytochemistry staining, a pluripotent stem cell 4-marker immunocytochemistry kit (Invitrogen), including primary antibodies against OCT4, SSEA4, SOX2 and TRA-1-60, was used to evaluate the pluripotency. Briefly, the experimental procedure was performed according to the manufacturer's instructions. For immunoblotting, whole cell lysates were prepared using RIPA lysis buffer containing 1% protease, 1% phosphatase, and 0.1% Triton X. The supernatant was collected after centrifugation at 12000 rpm for 30 min at 4 ℃. A total of 40 μg of total protein per sample was subjected to 10% SDS-PAGE and transferred to a PVDF membrane and subsequently blocked for 1 h with 5% bovine serum albumin in Tris-buffered saline containing 0.1% Tween 20 (TBST). The membranes were then incubated overnight with primary antibodies of different $pH_i$ regulators and an internal control at 4 ℃. Then, the membranes were washed three times in TBST to remove the unbound primary antibodies and the secondary antibody was then added and incubated for 60 min at room temperature. The membranes were washed three times in TBST, and chemiluminescence was detected using a Clarity™ Western ECL substrate.

### *Measurement of intracellular pH*

The measurement of the $pH_i$ has been described in detail in our previous reports[12]. Briefly, to measure the change in $pH_i$, HPS0077 hiPSCs were analyzed by microspectrofluorimetry with a pH-sensitive fluorescent dye, BCECF-AM. When cell colonies (on a 24 mm round coverslip) were grown to a sufficient size, cells were then incubated with BCECF-AM (diluted to 6.25 μg/mL with standard HEPES solution) for 1 h at room temperature. Then, the coverslip containing the cells was moved to an inverted fluorescence microscope and excited with light at wavelengths of 490 and 440 nm. The change in the BCECF emission ratio of the 530 nm wavelength emission at a 490 and 440 nm excitation (490/440) was detected and indicated the change in $pH_i$. A high potassium/nigericin calibration method was used to convert the emission ratio to the $pH_i$ value.

When the $pH_i$ was measured using a Synergy 2 Multi-Mode Reader, the cells were seeded on 24-well culture plates. The solution was replaced with a pipette instead of a perfusion system (including a peristaltic pump and suction). The experimental procedure is similar to microspectrofluorimetry, and the details are described in our previous study[23].

### *Weak acid/base prepulse technique*

$NH_4Cl$ and Na-acetate prepulse techniques were used to induce intracellular acidification and alkalization, respectively, and the subsequent recovery from induced acidification and alkalization represent the activity of the acid extruder(s) and acid loader(s), respectively[12]. Taking $NH_4Cl$ prepulse as an example, it can be described by 4 phases, as shown in Figure 1A. Cells were first perfused with 20 mmol/L $NH_4Cl$ for 5 min, which caused an initial rapid alkalization. This mechanism is simply caused by the small molecular weight and nonpolar $[NH_3]_e$ easily crossing the cell membrane and acquiring hydrogen in the cytosol to produce $NH_4^+$ (phase 1: rapid alkalization, $NH_3 + H^+ \rightarrow NH_4^+$). Then, the $pH_i$ slowly recovered and stabilized through the activation of acid loaders, such as AE and CHE (phase 2: slow recovery). The removal of $NH_4Cl$ caused rapid intracellular acidification because $[NH_3]_i$ rapidly effluxed and further produced hydrogen from $[NH_4^+]_i$ in the cytosol (phase 3: rapid acidification, $NH_4^+ \rightarrow NH_3 + H^+$). The subsequent $pH_i$ recovery following $NH_4Cl$-induced intracellular acidification is due to the activation of acid extruders, such as NHE and NBC, and this recovery slope represents the function of acid extruders (phase 4: $pH_i$ recovery). To accurately quantify the $H^+$ flux through $pH_i$ regulators, all $pH_i$ recovery rate data was converted to the $J_H$ ($pH_i$ recovery rate multiplied by buffering power)[10].

### *Measurement of intracellular buffering power to derive the net influx or the net efflux*

After the loading of BCECF-AM, cells were sequentially perfused with $Na^+/Cl^-$-free HEPES or 5% $CO_2/HCO_3^-$-buffered solution (the details of the composition of the solutions are listed in the *Solution* section below) containing different concentrations of $(NH_4)_2SO_4$ (40, 20, 10, 5, 2.5 and 0 mmol/L). Perfusion with $(NH_4)_2SO_4$ induced an initial intracellular alkalization, and the subsequent removal of $(NH_4)_2SO_4$ or decrease in $(NH_4)_2SO_4$ concentration caused acidification. The buffering power is defined as the ability to resist the change in $pH_i$ induced by the impact of hydrogen, *i.e.*, $(NH_4)_2SO_4$. Therefore, if the buffering power is stronger, the change in $pH_i$ will be smaller. The buffering power can be

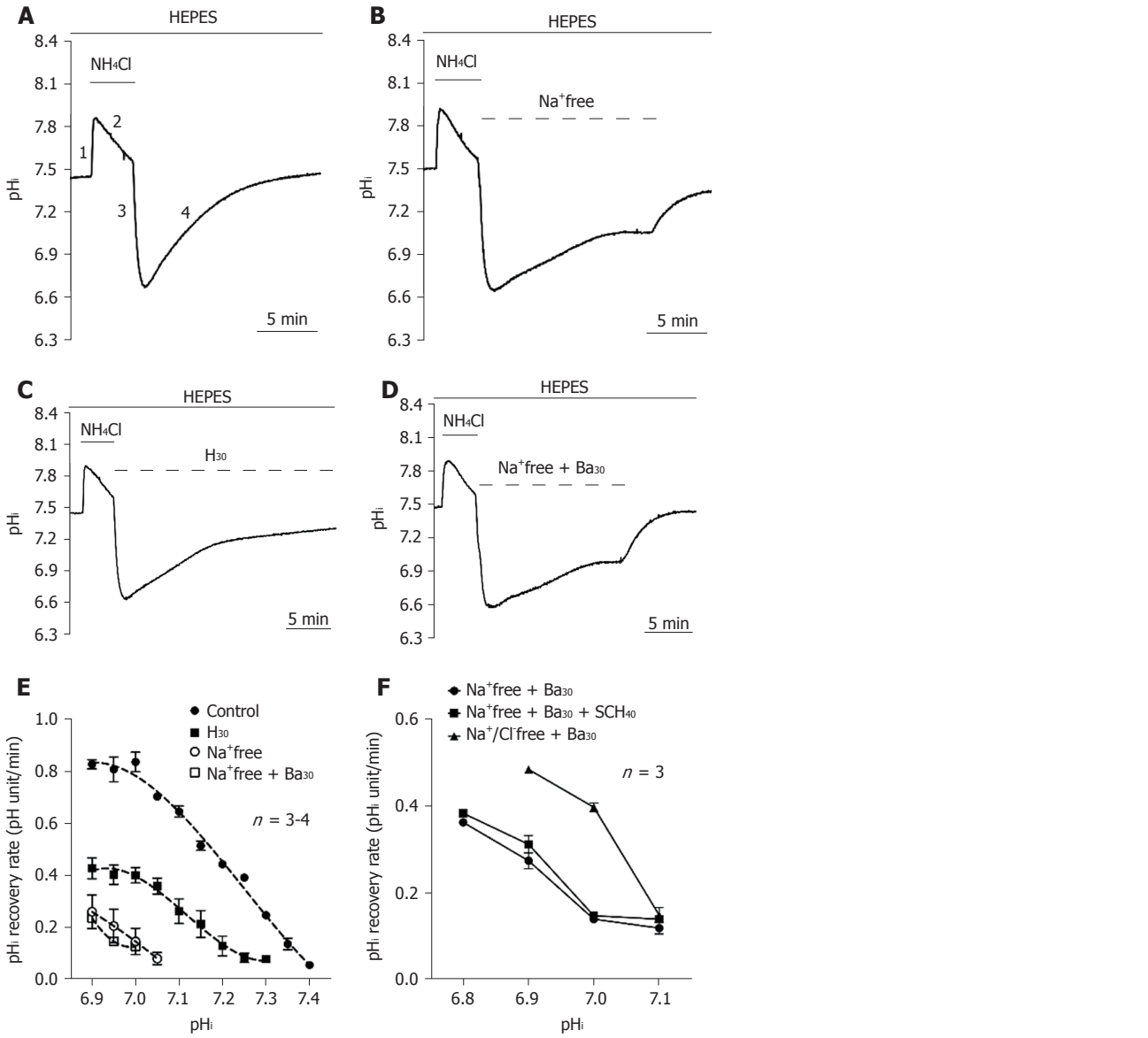


**Figure 1 Functional characterization of acid extruders in the HEPES-buffered system.** A-D: The top bar shows the buffer system used in perfusion experiments. The application of $NH_4Cl$ and different conditions were respectively shown with the solid and dotted lines above the trace. The trace shown in A showed a typical $pH_i$ recovery slope after $NH_4Cl$ prepulse-induced intracellular acidosis in HEPES-buffered solution as a control. The traces shown in B-D showed the effect of the removal of extracellular $Na^+$ ($Na^+$-free), addition of 30 μmol/L HOE 694 ($H_{30}$) and $Na^+$-free + 30 μmol/L bafilomycin A1 ($Ba_{30}$) on the $pH_i$ recovery slope. E: The curve of the $pH_i$ recovery rates for $Na^+$-free, $H_{30}$ and $Na^+$-free with $Ba_{30}$ were collected from 3-6 similar experiments shown in A-D. F: After pre-treatment with $NH_4Cl$ for 5 min, HPS0077 cells were treated with $Na^+$-free + $Ba_{30}$, $Na^+$-free + $Ba_{30}$ + 40 μmol/L SCH-28080 ($SCH_{40}$) and $Na^+/Cl^-$-free + $Na^+$-free + $Ba_{30}$ in HEPES-buffered solution, and the change in $pH_i$ was detected by a multimode reader. Error bars represent the mean ± SE.

defined by the following equation[38]:

$$\beta(mM) = [H^+]_i/\Delta pH_i, \quad (e.1)$$

Where $[H^+]_i$ is the change in the concentration of intracellular protons, and $\Delta pH_i$ is the resulting change in $pH_i$.

For experiments with the $NH_4Cl$ prepulse technique, the application of $(NH_4)_2SO_4$ externally induces intracellular alkalization. This is due to the rapid diffusion of $NH_3$ into the cell and its subsequent hydrogenation to form $NH_4^+$. Upon the removal of extracellular $(NH_4)_2SO_4$, $NH_4^+$ exits the cell as uncharged $NH_3$, leaving behind an equal concentration of $H^+$ and causing intracellular acidification. If $[H^+]_i$ is assumed to equal the intracellular concentration of $NH_4^+$ at the moment of their removal from the external solution, then equation 1 can be expressed as follows:

$$\beta(mM) = [NH_4^+]_i/\Delta pH_i. \quad (e.2)$$

According to the Henderson-Hasselbalch equation, the relationship between internal and external $NH_4^+$ concentration is as follows:

$$pH_o - pH_i = \log([NH_4^+]_i / [NH_4^+]_o). \quad (e.3)$$

Equation 3 can then be rearranged as follows:

$$[NH_4^+]_i = [NH_4^+]_o \times 10^{(pHo-pHi)}. \quad (e.4)$$

In the extracellular solution, $pH_o = pKa + \log([NH_3]_o/[NH_4^+]_o)$ (Henderson-Hasselbalch equation). Therefore, this equation can be rearranged as follows:

$$[NH_4^+]_o = C/(10^{(pHo-pK)} + 1), \quad (e.5)$$

where C is the total extracellular concentration of

$NH_4^+$ and pK is the dissociation constant of $(NH_4)_2SO_4$. Combining equations 4 and 5, we can derive $[NH_4^+]_i$ at a given $pH_i$ as follows:

$$[NH_4^+]_i = [C/(10^{(pHo-pK)} + 1)] \times 10^{(pHo-pHi)}. \quad (e.6)$$

In an open system, the theoretical $\beta_{CO2}$ can be calculated as follows:

$$\beta_{CO2} = 2.3 \times [HCO_3^-]_i. \quad (e.7)$$

Similar to the calculation procedures outlined above for $NH_4^+$, $[HCO_3^-]_i$ can then be calculated as follows:

$$[HCO_3^-]_i = [C/(10^{(pK-pHo)} + 1)] \times 10^{(pHi-pHo)}. \quad (e.8)$$

### *Solutions and chemicals*

Nigericin calibration solution was composed of 140 mmol/L KCl, 1 mmol/L $MgCl_2$, 0.01 mmol/L nigericin and 10 mmol/L buffer (MES, HEPES or CAPSO), and the pH was adjusted to 5.5, 6.5, 7.0, 7.5, 8.5 or 9.5 with 6 mol/L NaOH. The buffers used in the calibration solution were in accordance with the pKa of the buffers and the pH of the solution (MES was used for pH = 5.5 and 6.5; HEPES was used for pH = 7.0, 7.5 and 8.5; and CAPSO was used for pH = 9.5).

Standard HEPES-buffered solution was composed of 140 mmol/L NaCl, 4.5 mmol/L KCl, 1 mmol/L $MgCl_2$, 2.5 mmol/L $CaCl_2$, 11 mmol/L glucose, and 20 mmol/L HEPES. Standard bicarbonate-buffered Tyrode's solution (equilibrated with 5% $CO_2$/22 mmol/L $HCO_3^-$) was the same as above, except that the NaCl concentration was reduced to 117 mmol/L, and 22 mmol/L $NaHCO_3$ was added instead of HEPES (pH 7.40 at 37 ℃).

**Ion-substituted solutions:** For $Na^+$-free HEPES-buffered Tyrode's solution, NaCl was replaced with 140 mmol/L N-methyl-D-glucamine (NMDG). For $Cl^-$-free $CO_2/HCO_3^-$-buffered Tyrode's solution contained 117 mmol/L sodium gluconate, 4.5 mmol/L potassium gluconate, 12 mmol/L calcium gluconate, 22 mmol/L $NaHCO_3$, 1 mmol/L $MgSO_4$, and 11 mmol/L glucose. The $Na^+/Cl^-$-free solution (for the buffering power experiment) was composed of 140 mmol/L NMDG, 4.5 mmol/L K-gluconate, 1 mmol/L Mg-gluconate, 2.5 mmol/L Ca-gluconate, 11 mmol/L glucose and 20 mmol/L HEPES (for 5% $CO_2/HCO_3^-$-free system) or bubbled with 5% $CO_2$ (for 5% $CO_2/HCO_3^-$ system). The pH was adjusted to 7.4 with 6 mol/L NaOH, HCl or $H_2SO_4$ at 37 ℃ for all solutions. $NH_4Cl$, Na-acetate and $(NH_4)_2SO_4$ were directly added as solids to the buffered solutions before use. HOE 694 (HOE, a NHE1 specific inhibitor), S0859 (an NBC-specific inhibitor), bafilomycin A1 (Ba, a V-type ATPase-specific inhibitor) and SCH-28080 (SCH, a KHE-specific inhibitor) were added as stocks to solutions shortly before use. All drugs mentioned above were obtained from Sigma-Aldrich.

### *Statistical analysis*

The data were expressed as the mean ± SE of *n* preparations. The statistical significance was analyzed using one-way or two-way ANOVA followed by Tukey's or Dunnett's multiple comparisons with GraphPad Prism 6 software, respectively. A *P*-value less than 0.05 were regarded as statistically significant.

## RESULTS

### *In situ calibration of BCECF and the detection of hiPSC pluripotency markers*

To monitor the change in $pH_i$, an *in situ* calibration was conducted in hiPSCs. A high potassium/nigericin calibration method was used to convert the emission ratio to the $pH_i$ value. Briefly, BCECF-loaded cells were perfused with six different nigericin calibration solutions with different pH levels (5.5-9.5) (the details of the composition of the six nigericin calibration solutions are listed above in the solutions section) that caused the $pH_i$ to equal the $pH_e$, as shown in Figure 2A. The calibration equation was obtained from ten similar experiments and a nonlinear BCECF fluorescence-$pH_i$ curve of function, as shown below and in Figure 2B. The following equation was used to convert the fluorescence ratio into $pH_i$:

$$pH_i = pK_a + \log[(R_{max} - R)/(R - R_{min})] + \log(F_{440min}/F_{440max})$$

Where R is the ratio of the 530 nm fluorescence emission at 490 nm and 440 nm excitation (490/400), and F is the fluorescence value at 490 nm and 440 nm excitation. The maximum and minimum ratios ($R_{max}$ and $R_{min}$) of 530/490 and 530/440 (Em/Ex) were obtained from perfusion with pH 9.5 and 5.5 calibration solutions, respectively.

Because the HPS0077 cell line was used as a representative example of hiPSCs in this study, we first examined whether pluripotency markers, such as OCT4, SOX2, SSEA-4 and TRA-1-60, are present in HPS0077 cells. As shown in Figure 2C, the four pluripotency markers were clearly identified by immunofluorescence staining and labeling. Our results support the hypothesis that the HPS0077 cell line possesses the characteristics of hiPSCs and is suitable as the subject for this study.

### *Functional characterization of acid extruders in HEPES buffered system*

To investigate whether there is an acid extrusion mechanism in the cultured hiPSCs, the cells were first perfused in HEPES-buffered solution ($CO_2/HCO_3^-$-free). As shown in Figure 1A, a $pH_i$ recovery slope following $NH_4Cl$ prepulse-induced intracellular acidification was a typical trace for the control ($n$ = 3). Either removal of the extracellular $Na^+$ ($n$ = 3) or application of 30 μmol/L HOE 694 ($H_{30}$, $n$ = 4) significantly inhibited the $pH_i$ recovery rate, as shown in Figures 1B and 1C, respectively, which demonstrates the presence of $Na^+$-dependent acid extruder(s) and NHE1 in HPS0077 cells.

However, besides $Na^+$-dependent acid extruders, there is another acid extrusion mechanism responsible for the remaining acid extrusion in HEPES solution. Therefore, to further investigate whether the remai-

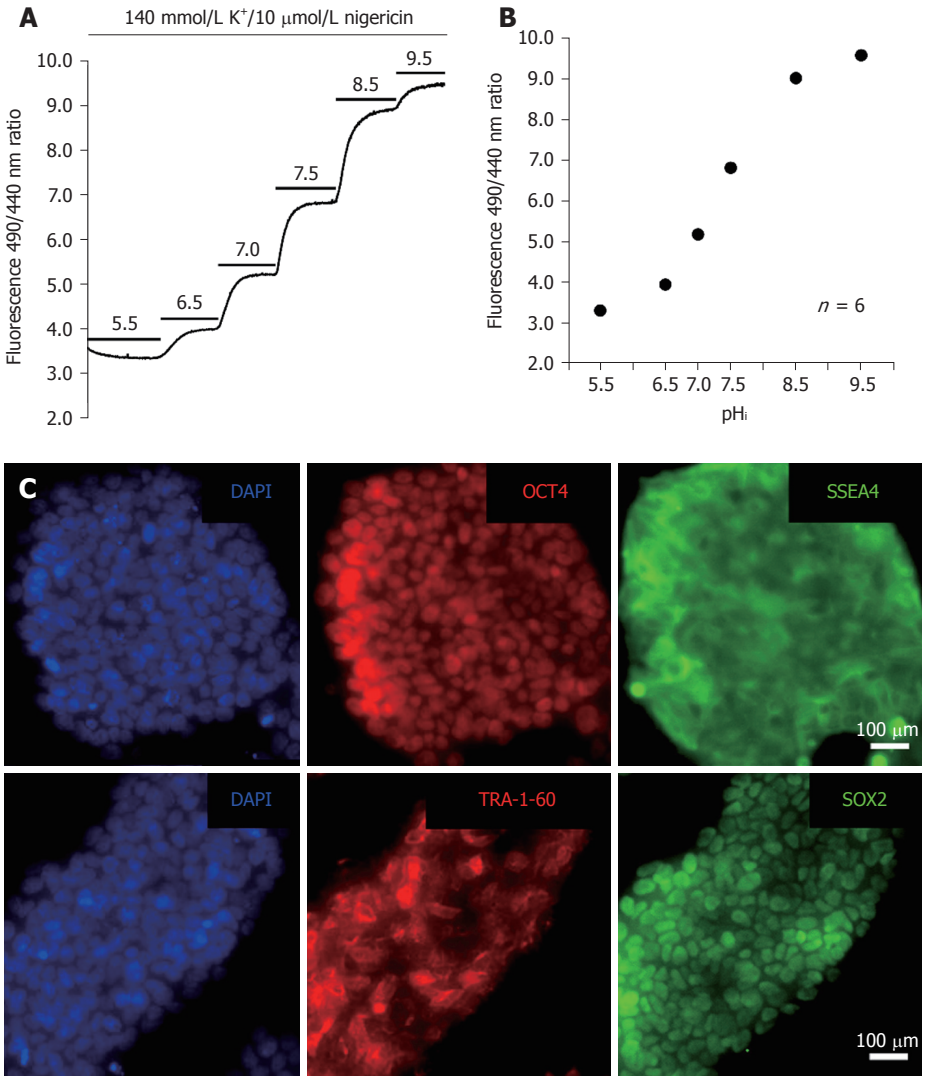


**Figure 2 Calibration of the BCECF fluorescence ratio and pluripotency characterization.** A: The trace showed the protocol of BCECF fluorescence ratio (510 nm emission at 490 nm and 440 nm excitations) calibration in HPS0077 cells. The top bars represent the application of different conditions; B: The plots of $pH_i$ *vs* the BCECF fluorescence ratio were collected from 6 similar experiments shown in A; C: Immunofluorescence analysis showed the expression of pluripotency markers, OCT4, SSEA4, TRA-1-60 and SOX2, in HPS0077 cells.

ning $Na^+$-independent $pH_i$ recovery (*i.e.*, could not be inhibited by $Na^+$-free solution) is caused by the vacuolar-type ATPase (V-ATPase), HPS0077 cells were perfused with an $Na^+$-free solution pulse with 30 μmol/L bafilomycin A1 ($Ba_{30}$; V-ATPase-specific inhibitor, $n$ = 3), as shown in Figure 1D. However, either no significant inhibition or slight inhibition of $pH_i$ recovery was observed between the $Na^+$-free solution group and the $Na^+$-free solution + $Ba_{30}$ group (Figures 1B and 1D, respectively). These results suggest that V-ATPase does not play a role in acid extrusion to the cytosol in hiPSCs. Experimental data similar to those shown in Figures 1A-D were summarized and plotted as a function of the $pH_i$ recovery rate *vs* $pH_i$ in Figure 1E. As shown in Figure 1E, in HEPES solution (*i.e.*, when $HCO_3^-$-dependent acid extruder(s) were not activated), the acid extrusion mechanism was mainly attributed to NHE1 (the difference between the trace of the $Na^+$-free group and the trace of the $H_{30}$ group), apart from other $Na^+$-dependent acid extruder(s) (the difference between the trace of $H_{30}$ and the trace of $Na^+$-free). Moreover, the other $Na^+$-independent acid extruder(s) were activated when the $pH_i$ was less than 7.1 ± 0.01 (see the trace of $Na^+$-free + $Ba_{30}$).

To further examine whether the $Na^+$-independent acid extruders shown in Figure 1E are KHE or $Cl^-$-dependent acid extruder(s), HPS0077 cells were either performed by adding 40 μmol/L SCH-28080 ($SCH_{40}$, a KHE-specific inhibitor) or removing $[Cl^-]_o$. The change in $pH_i$ in this series of experiments was detected using a Synergy 2 Multi-Mode Reader with BCECF-AM dye. The data for this series of experiments were summarized and plotted as a function of the $pH_i$ recovery rate *vs* $pH_i$ in Figure 1F. As shown in Figure 1F, the $pH_i$ recovery rate between the trace before and after adding $SCH_{40}$ ($n$ = 3, solid circles and squares, respectively) was not significantly different. Moreover, the removal of $[Cl^-]$ ($n$ = 3, solid triangles) surprisingly caused a dramatic

increase in the $pH_i$ recovery rate instead of inhibition. This phenomenon is most likely caused by the inhibition of the activity of the $Cl^-$-dependent acid loader. In summary, these results provide clear pharmacological evidence that the NHE is mainly responsible for acid extrusion and functionally coexists with other $Na^+$-dependent and -independent acid extrusion mechanisms in HPS0077 cells. Moreover, the $Na^+$-independent acid extrusion mechanism is neither a KHE nor a $Cl^-$-dependent acid extruder(s).

### *Functional characterization of acid extruders in a 5% $CO_2/HCO_3^-$-buffered system*

To quantify the $[H_i]^+$ flux through $pH_i$ regulators in 5% $CO_2/HCO_3^-$-buffered conditions, we first quantified intracellular buffering ($\beta$). The experimental details are shown in the materials and methods section, and we found that $\beta$ increased as $pH_i$ increased at $pH_i$ = 7.0 to 8.0 ($n$ = 35, data not shown). The equation can be expressed as $\beta = 107.79\ (pH_i)^2 - 1522.2\ (pH_i) + 5396.9$ (correlation coefficient $R^2 = 0.85$). The obtained $\beta$ can be used to calculate the $[H_i]^+$ flux through $pH_i$ regulators by the following equation: $J_H = \beta \times pH_i$ recovery rate ($pH_i$ value/minutes). To further investigate whether the NBC is functionally involved in the 5% $CO_2/HCO_3^-$ condition, we used a protocol similar to the previously mentioned experiments except for the replacement of HEPES-buffered solution with 5% $CO_2/HCO_3^-$-buffered solution. The $pH_i$ recovery slope following $NH_4Cl$ prepulse-induced intracellular acidification in 5% $CO_2/HCO_3^-$-buffered solution was a typical trace for the control ($n$ = 7), as shown in Figure 3A. As shown in Figures 3B-E, the $pH_i$ recovery rate was significantly inhibited under four different conditions as follows: removal of $[Na^+]$ ($n$ = 3, addition of $H_{30}$ ($n$ = 4), addition of 90 μmol/L S0859 ($S_{90}$; an inhibitor of NBC, $n$ = 3), and addition of $H_{30}$ and $S_{90}$ ($H_{30}$ + $S_{90}$, $n$ = 3). Experimental data similar to those shown in Figures 3A-E were summarized and plotted as a function of $J_H$ *vs* $pH_i$ in Figure 3F. As shown in Figure 3F, a similar $pH_i$ recovery rate between $Na^+$-free and $H_{30}$ + $S_{90}$ conditions indicated that the NHE1 and the NBC were both involved in the $Na^+$-dependent acid extrusion mechanism in the 5% $CO_2/HCO_3^-$ condition in HPS0077 cells.

Notably, the acid extrusion mechanism in the 5% $CO_2/HCO_3^-$ condition was regulated mainly by the NBC in the $pH_i$ range of 7.50-7.68 because the $pH_i$ recovery rate could be completely inhibited by $S_{90}$ (Figure 3D). Moreover, the addition of $S_{90}$ did not affect $pH_i$ recovery when the $pH_i$ was less than 6.9 ± 0.01 ($n$ = 3, see the trace of $S_{90}$), which indicated that the NBC was not responsible for acid extrusion in the relatively acidic cytoplasm (Figure 3D). In summary, NHE1, NBC and $Na^+$-independent acid extruder(s) were mainly functionally activated in the $pH_i$ ranges of < 7.5, 6.9-7.68 and < 7.1, respectively.

### *Functional characterization of acid loaders*

The homeostasis of $pH_i$ is coregulated by both acid extruders and acid loaders. The CHE and the AE are two known acid loaders in mammalian cells. Unlike the NHE and the NBC, the acid loading mechanism depends on $[Cl^-]_o$ and further exchange of $[OH^-]_i$ or $[HCO_3^-]_i$ out of the cytoplasm to neutralize intracellular alkalization. To estimate the function of acid loaders, an Na-acetate prepulse was used to induce intracellular alkalization in this study. The subsequent $pH_i$ recovery slope was expressed as the acid loading activity of acid loaders. Figures 4A and 4C show the typical $pH_i$ recovery slope following the Na-acetate prepulse either in HEPES or $HCO_3^-$-buffered solution, respectively ($n$ = 3). Removal of $[Cl^-]_o$ in the 5% $CO_2/HCO_3^-$-buffered solution completely inhibited the $pH_i$ recovery ($n$ = 3), as shown in Figure 4D, which indicated that the acid loading mechanism is completely $Cl^-$-independent in HPS0077 cells. However, interestingly, a rapid acid loading phenomenon was observed before the total inhibition at $pH_i$ = 7.9 ± 0.01 ($n$ = 3) in HEPES solution, as shown in Figure 4B. These results indicated that $CO_2$ or $HCO_3^-$ may inhibit this unknown $Cl^-$-dependent acid loader(s), but the characterization requires further studies. Due to the lack of specific inhibitors of the CHE and the AE, according to previous studies on the acid loading mechanism in mammalian cells conducted by Leem *et al*[39], we speculate that the $Cl^-$-independent acid loading mechanism is mainly attributed to the CHE and the AE[39]. Notably, as shown in Figure 4E, the $pH_i$ recovery rate is nearly identical between the 5% $CO_2/HCO_3^-$ system (solid circles) and the HEPES system (solid squares), which indicates that the CHE plays a more important role than the AE in the acid loading mechanism in HPS0077 cells.

### *Decrease in $pH_i$ during the loss of pluripotency: molecular and functional evidence*

Our previously mentioned results showed that the acid extruders NHE and NBC mainly functionally coexist in hiPSCs.

We further investigated the dynamic changes in $pH_i$ during the loss of pluripotency in hiPSCs. In the pluripotent state, the resting $pH_i$ observed from the $pH_i$ completely recovered after $NH_4Cl$ prepulse-induced intracellular acidification was found to be 7.5 ± 0.01 ($n$ = 20) and 7.68 ± 0.01 ($n$ = 20) in HEPES and 5% $CO_2/HCO_3^-$ conditions, respectively, as shown in Figures 5A and 5B. Moreover, in 5% $CO_2/HCO_3^-$-buffered solution, as expected, the resting $pH_i$ shifted to 7.46 ± 0.02 ($n$ = 5) and 7.66 ± 0.02 ($n$ = 5) after adding S0859 ($S_{90}$) and HOE694 ($H_{30}$), respectively (Figure 5B, the data were collected from the data shown in Figures 3C and 3D). Notably, there was no significant difference between the resting $pH_i$ in HEPES and in the 5% $CO_2/HCO_3^-$ plus $S_{90}$ conditions, which indicates that the set-point of NHE activation is $pH_i$ = 7.5. In the 5% $CO_2/HCO_3^-$ condition, the resting $pH_i$ showed no significant difference between the untreated and $H_{30}$-treated conditions, which indicates that the $pH_i$ is regulated by the NBC instead of the NHE in the $pH_i$ range of 7.50-7.68.

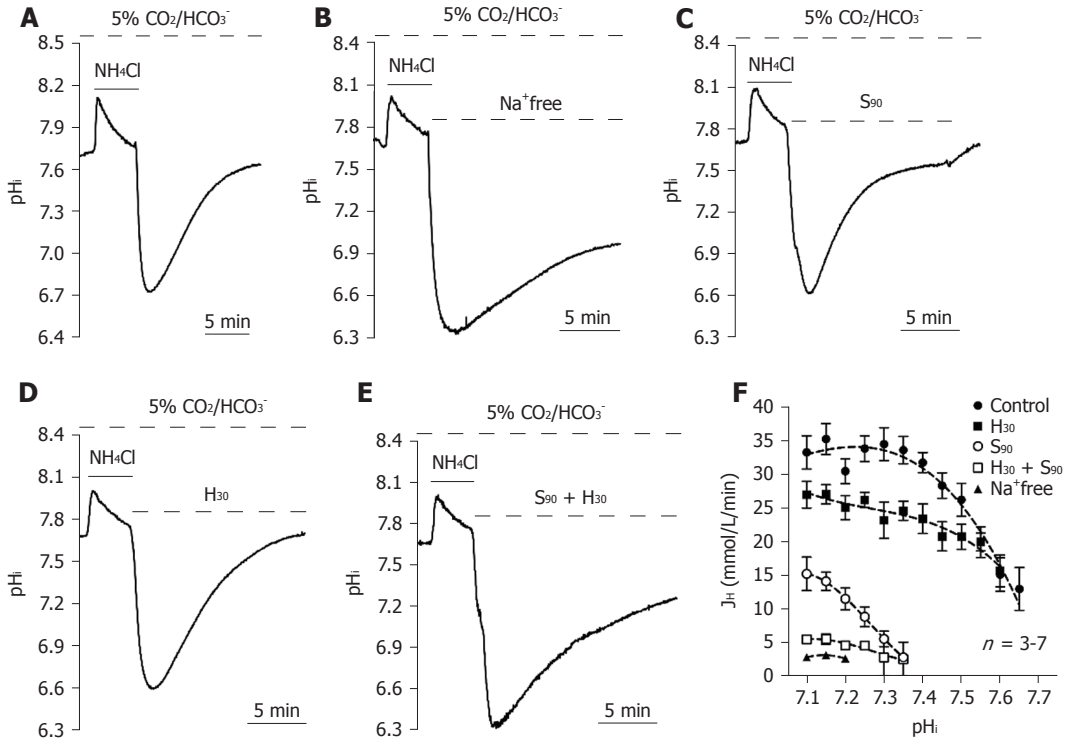


**Figure 3 Functional characterization of acid extruders in the 5% $CO_2/HCO_3^-$-buffered system.** A-E: The trace shown in A showed a typical $pH_i$ recovery slope after $NH_4Cl$ prepulse-induced intracellular acidosis in HEPES-buffered solution as a control. The traces shown in B-E showed the effect of the removal of extracellular $Na^+$ ($Na^+$-free), addition of 90 μmol/L S0859 ($S_{90}$), addition of 30 μmol/L HOE 694 ($H_{30}$) and addition of $S_{90}$ + $H_{30}$ on the $pH_i$ recovery slope; F: The curve of the $pH_i$ recovery rates after the addition of $Na^+$-free, $S_{90}$, $H_{30}$ and $S_{90}$ + $H_{30}$ were collected from 2-10 similar experiments shown in A-E. Error bars represent the mean ± SE.

To further induce the loss of pluripotency, HPS0077 cells were first transferred from mTeSR1 media (designed for maintaining long-term pluripotency) to mTeSR-E8 medium (containing fibroblast growth factor 2, FGF2, and transforming growth factor β1, TGFβ1) and then subsequently replaced with mTeSR-E6 medium (without FGF2 and TGFβ1) for 1 to 4 days (E6-1d to 4d) to induce the loss of pluripotency. Notably, the expression of the pluripotency marker OCT4 was significantly decreased after culture in mTeSR-E6 medium, as shown in Figure 5C. We also found that the expression of NHE1, NHE3, V-ATPase, NBCe1 and NBCe2 decreased during the loss of pluripotency, while the expression of NBCn1 did not decrease, as shown in Figure 5C.

To further investigate the role of the NHE and the NBC on the loss of pluripotency, we detected the $pH_i$ recovery rate following $NH_4Cl$ prepulse-induced intracellular acidification. The $pH_i$ recovery traces in different culture mediums, *i.e.*, E8, E6-1d, E6-2d, E6-3d and E6-4d in HEPES and 5% $CO_2/HCO_3^-$-buffered solution are shown in Figures 6A and 6D, respectively. The graphs in Figure 6B show the $pH_i$ recovery rate in E6-1d to E6-4d normalized from the E8 condition (% of E8) in HEPES, estimated at $pH_i$ = 6.9 and 7.2, respectively, and averaged for 3 experiments similar to that shown in Figure 6A. The NHE is mainly responsible for acid extrusion in the HEPES condition. When the $pH_i$ recovery rate was measured at $pH_i$ = 6.9, E6-1d showed no significant change, while E6-2d, E6-3d and E6-4d significantly decreased by 76.3%, 60.6% and 51.7%, respectively ($n$ = 3). When the $pH_i$ recovery rate was measured at $pH_i$ = 7.2, the $pH_i$ recovery rates of E6-1d, E6-2d, E6-3d and E6-4d significantly decreased by 82.7%, 67.4%, 47.6% and 16.3%, respectively ($n$ = 3). The max/min charts in Figure 6C show the resting $pH_i$ in E8, E6-1d, E6-2d, E6-3d and E6-4d, respectively, averaged from similar experiments as shown in Figure 6A ($n$ = 5-20). The resting $pH_i$ decreased from 7.5 to 7.49, 7.4, 7.28 and 7.21 in E6-1d, E6-2d, E6-3d and E6-4d, respectively ($n$ = 5 to 20).

The graphs shown in Figure 6E show the $pH_i$ recovery rate in E6-1d to E6-4d normalized to E8 (control) in 5% $CO_2/HCO_3$-buffered solution, which was estimated at $pH_i$ = 6.9, 7.2 and 7.5, respectively, and averaged for 3 experiments similar to that shown in Figure 6D. As shown in Figure 6E, in the 5% $CO_2/HCO_3^-$ condition (*i.e.*, where the NHE and the NBC were both involved in the acid extrusion mechanism), the $pH_i$ recovery rate measured at $pH_i$ = 6.9 and 7.2 showed no significant difference between E8 and E6-1d, but it was significantly decreased by 85.2% when measured at $pH_i$ = 7.5. The $pH_i$ recovery rate for E6-2d, E6-3d and E6-4d was significantly decreased by 88.7, 74.9 and 61%, respectively, when measured at $pH_i$ = 6.9, decreased by 82%, 77.2% and 51.5%, respectively, when measured at $pH_i$ = 7.2, and decreased by 53.4%, 44.8% and 22.3%, respectively, when measured at $pH_i$ = 7.5 ($n$ = 3). The max/min charts shown in Figure 6F show the resting $pH_i$ in E8, E6-1d, E6-2d, E6-3d and E6-4d, averaged from similar experiments as those shown

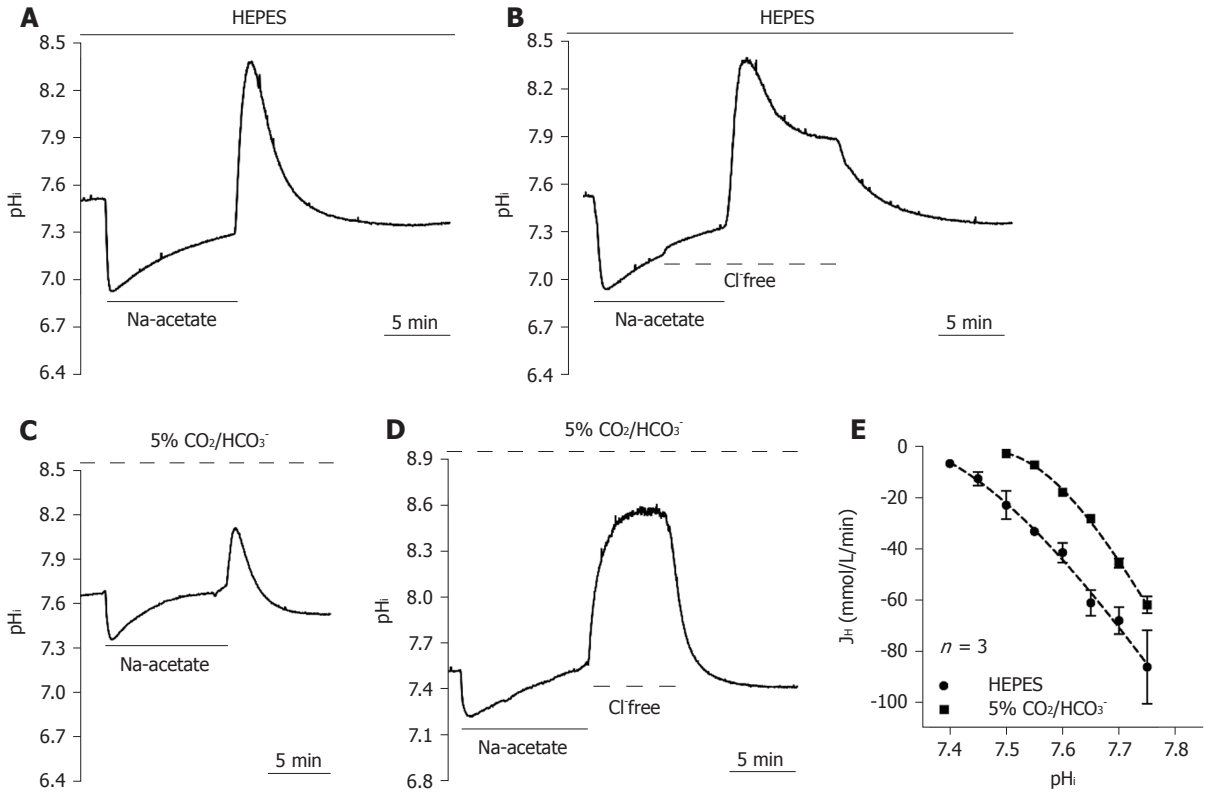


**Figure 4 Functional characterization of the acid loader.** A-D: The traces shown in A and C showed typical $pH_i$ recovery slopes after Na-acetate prepulse-induced intracellular alkalization in HEPES and 5% $CO_2/HCO_3^-$-buffered solution as a control. The traces shown in B and D showed the effect of the removal of extracellular $Cl^-$ ($Cl^-$-free) on the $pH_i$ recovery slope in HEPES and 5% $CO_2/HCO_3^-$-buffered solution; E: The curve of the $pH_i$ recovery rates in HEPES and 5% $CO_2/HCO_3^-$-buffered solution were collected from 3-4 similar experiments shown in A and C. Error bars represent the mean ± SE.

in Figure 6D ($n$ = 5-20). We found that the resting $pH_i$ decreased from 7.68 to 7.64, 7.61, 7.56 and 7.48 in E6-1d, E6-2d, E6-3d and E6-4d, respectively ($n$ = 5, Figure 6F). In summary, our results provide clear evidence that the loss of hiPSC pluripotency decreased the activity and expression of acid extruders (NHE and NBC), further resulting in a decrease in the $pH_i$ recovery rate and resting $pH_i$.

## DISCUSSION

### *The functional and molecular evidence of active transmembrane acid extruders and acid loaders in hiPSCs*

In this study, we have clearly demonstrated that transmembrane active $pH_i$ regulators, such as NHE1, NBC, AE and CHE, functionally coexisted in hiPSCs (Figures 3 and 4). Moreover, we successfully quantified the net acid efflux of each functional acid transporter, as shown in Figures 3 and 7, by considering intracellular buffering. From Figure 3F, we can clearly observe that the active efflux was mainly dependent on the activity of the NBC in hiPSCs in the $pH_i$ range less than 7.35 because the $S_{90}$ group (*i.e.*, inhibiting NBC activity) substantially decreased the activity compared to other groups (inhibiting NHE1 or other Na-independent acid extruders). Moreover, the role of NHE1 on acid extrusion decreased as the $pH_i$ increased (Figures 1, 3 and 7). Notably, the activity of NHE1 was nominally undetectable when the $pH_i$ was greater than 7.50, as shown in Figures 1, 3 and 7.

Relevant molecular candidates for the NBC include at least five members of the slc4 family, including 2 electrogenic $Na^+$-$HCO_3^-$ cotransporters (NBCe1/SLC4A4 and NBCe2/SLC4A5), 1 electroneutral $Na^+$-$HCO_3^-$ cotransporter (NBCn1/SLC4A7) and 2 $Na^+$-dependent $Cl^-$-$HCO_3^-$ exchangers (NCBE/SLC4A10 and NDCBE/SLC4A8)[7,40,41]. In this study, we found that three isoforms of the NBC, NBCn1, NBCe1 and NBCe2, coexist in hiPSCs, which is similar to our previously reported results in cultured human renal artery smooth muscle cells[7]. However, the Aalkjaer group has demonstrated that the NBC is NBCn1, *i.e.*, it is electroneutral, in rat and mouse smooth muscle cells[42], which is similar to the results reported in guinea pig myocytes by the Vaughan-Jones group[10]. In other words, the coexistence of 3 types of NBCs in hiPSCs is different from the results in mouse and rat models (c.f. Aalkjaer's group) and guinea pig models (c.f. Vaughan-Jones's group, which is likely due to differences in species/organs.

Moreover, in contrast to the results reported in our previous studies in cardiovascular cells, we found that $Na^+$-independent acid extruder(s) and $Cl^-$-independent acid loader(s) were substantially present for acid extrusion ($pH_i$ < 7.1) and acid loading ($pH_i$ > 7.9) in hiPSCs (Figures 1, 4 and 7). We further demonstrated

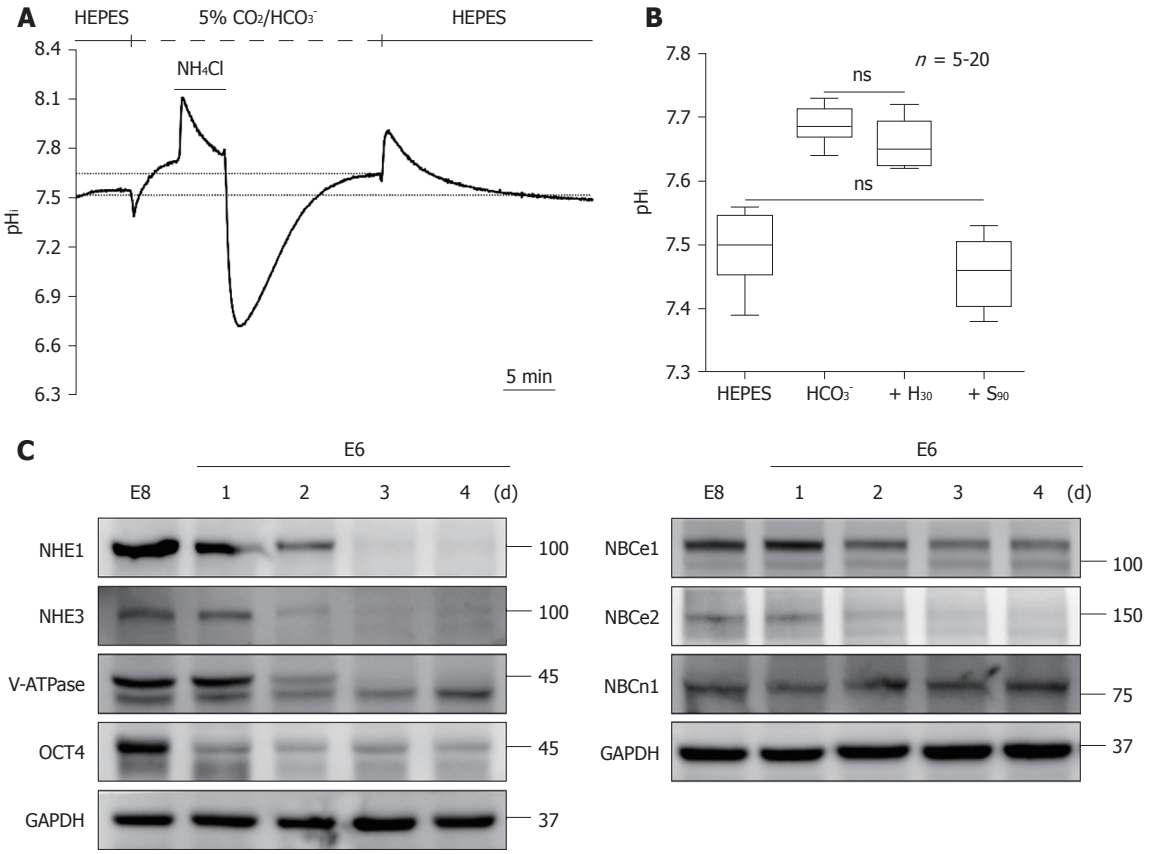


**Figure 5 Steady-state pHi in HEPES and 5% $CO_2/HCO_3^-$-buffered solution and the change in the expression of pHi regulators during the loss of pluripotency in human induced pluripotent stem cells.** A: The resting pHi was a steady-state taken from the completely recovered pHi after intracellular acidification or alkalization. The dotted line indicates the value of the resting pHi; B: The max/min chart of the resting pHi in hiPSCs was collected from A ($n$ = 20) and Figures 4C and D ($n$ = 5). The means of the resting pHi in HEPES and 5% $CO_2/HCO_3^-$-buffered solution were found to be 7.50 ± 0.01 and 7.68 ± 0.01, respectively. After treatment with $H_{30}$ and $S_{90}$ in 5% $CO_2/HCO_3^-$-buffered solution, the resting pHi shifted to 7.66 ± 0.02 and 7.46 ± 0.02, respectively; C: Immunoblot analysis of the expression of NHE1, NHE3, V-ATPase, NBCe1, NBCe2, NBCn1 and OCT4 in hiPSCs in different culture media for different days (E8 and E6-1d to E6-4d). The histograms in B display the mean and the min to max values. hiPSCs: Human induced pluripotent stem cells; NHE: The $Na^+/H^+$ exchanger; NBC: The $Na^+/HCO_3^-$ cotransporter; V-ATPase: Vacuolar-ATPase.

that the unknown $Na^+$-independent acid extruder(s) is not the V-ATPase, KHE[43] or $Cl^-$-dependent acid extruder (localized on lysosome and gastric cell membranes)[44,45] (Figures 1D and 1F). Therefore, we hypothesize that this unknown $Na^+$-independent mechanism is most likely an ATP-dependent transporter instead of a concentration gradient-driven transporter. For example, ATP deficiency, induced by the addition of oligomycin, combined with the addition of bafilomycin A1 during the perfusion experiments would allow us to observe whether it inhibits $Na^+$/V-ATPase-independent acid extrusion in hiPSCs[46]. However, functional and molecular characterization requires further studies in the future.

In addition to being an acid extruder, NBCe1 has been reported to be responsible for the acid loading mechanism during the process of changing from the HEPES-buffered solution to the 5% $CO_2/HCO_3^-$-buffered solution in mouse astrocytes[47]. However, in our findings, the addition of 50 μM S0859 still failed to inhibit the $Cl^-$-independent acid extrusion mechanism in the HEPES-buffered condition (data not shown). This result suggested that the $Cl^-$-independent acid extruder(s) was not NBCe1 in hiPSCs. Due to this unknown $Cl^-$-independent acid extrusion mechanism being completely inhibited in the $CO_2/HCO_3^-$-buffered system and the lack of related studies, future works should further characterize the possible existence of a $CO_2$-related pHi acid loading mechanism.

### *The implication of the existence of extra acid extrusion/loading mechanisms in hiPSCs*

The existence of an unknown acid extrusion mechanism, *i.e.*, $Na^+$-independent acid extruder(s) (see Figure 3F) and acid loading mechanisms, *i.e.*, $Cl^-$-independent acid loader(s), in hiPSCs might imply that the ability to resist the acid/base impact is very important for the pluripotency of hiPSCs[37,48,49]. It has been reported that hiPSCs share many cellular properties with cancer cells, such as increased cell proliferation and dependence on glycolysis for metabolism[24,26,50,51]. Many studies showed that a lower pHi decreased proliferation and energy production in either normal or cancer cells[15,26]. Indeed, in this study, we found that the acid extrusion mechanism was fully activated at an acidic pHi (< 7.2), including the NHE, the NBC

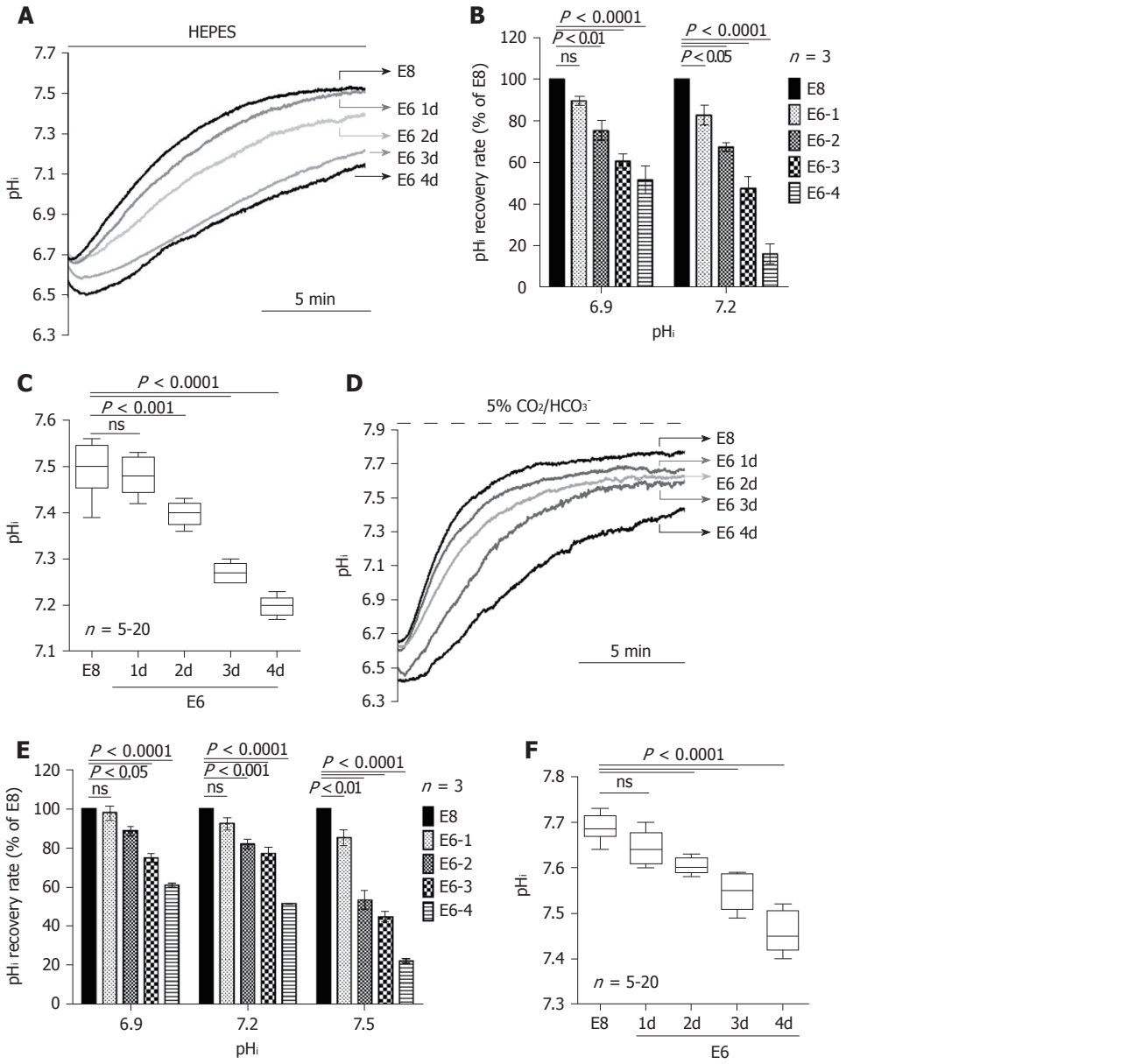


**Figure 6 The change in the activity of the $Na^+/H^+$ exchanger and the $Na^+/HCO_3^-$ cotransporter and the resting $pH_i$ during the loss of pluripotency in human induced pluripotent stem cells.** A: The traces showed the changes in $pH_i$ recovery after $NH_4Cl$ prepulse-induced intracellular acidification in E8 medium (containing fibroblast growth factor 2, FGF2, and transforming growth factor β1, TGFβ1) and E6 medium (without FGF2 and TGFβ1) for 1 to 4 d (E6-1d to E6-4d) in HEPES-buffered solution; B: The charts showed the $pH_i$ recovery rate in E6-1d to -4d normalized to the rate in E8 (% of E8) in HEPES-buffered solution, which was estimated at $pH_i$ = 6.9 and 7.2, respectively, and averaged for 3 experiments similar to that shown in A; C: The max/min plots showed the resting $pH_i$ in E8, E6-1d, E6-2d, E6-3d and E6-4d media that were averaged from similar experiments shown in A ($n$ = 5-20); D: The traces showed the changes in $pH_i$ recovery after $NH_4Cl$ prepulse-induced intracellular acidification in E8 and E6-1d to E6-4d media in 5% $CO_2/HCO_3^-$-buffered solution; E: The graphs show the $pH_i$ recovery rate in E6-1d to E6-4d normalized to the rate in E8 (control) in 5% $CO_2/HCO_3^-$-buffered solution, which was estimated at $pH_i$ = 6.9, 7.2 and 7.5, respectively, and averaged for 3 experiments similar to that shown in D; F: The max/min plots showed the resting $pH_i$ in E8 E6-1d, E6-2d, E6-3d and E6-4d media, averaged from similar experiments shown in D ($n$ = 5-20). Error bars represent the mean ± SE. The histograms in C and F show the mean and min to max values. NS: No significant difference; hiPSCs: Human induced pluripotent stem cells.

and an unknown $Na^+$-independent acid extruder(s), in hiPSCs. As expected, the resting $pH_i$ in hiPSCs was found to be 7.5 and 7.68 in the HEPES and 5% $CO_2/HCO_3^-$ conditions, respectively, and was relatively higher than that of normal differentiated adult cells (resting $pH_i$ = 6.9-7.2), such as cardiovascular cells and tissues demonstrated in our previous studies[7,13,52,53]. In cancer, the reversal of the intracellular/extracellular pH ($pH_i/pH_e$) gradient (alkaline $pH_i$ and acidic $pH_e$) is a common feature and further promotes carcinogenesis. The reason for the gradient reversal is that cancer cells overexpress and upregulate the set-point of acid extruders[24-26]. Therefore, it is likely that hPSCs may upregulate the acid extrusion mechanism to adapt to cancer-like cellular properties. Some studies showed that, in addition to hiPSC growth being inhibited by an acidic culture environment, the alkalization of culture medium significantly decreases the cell growth rate and

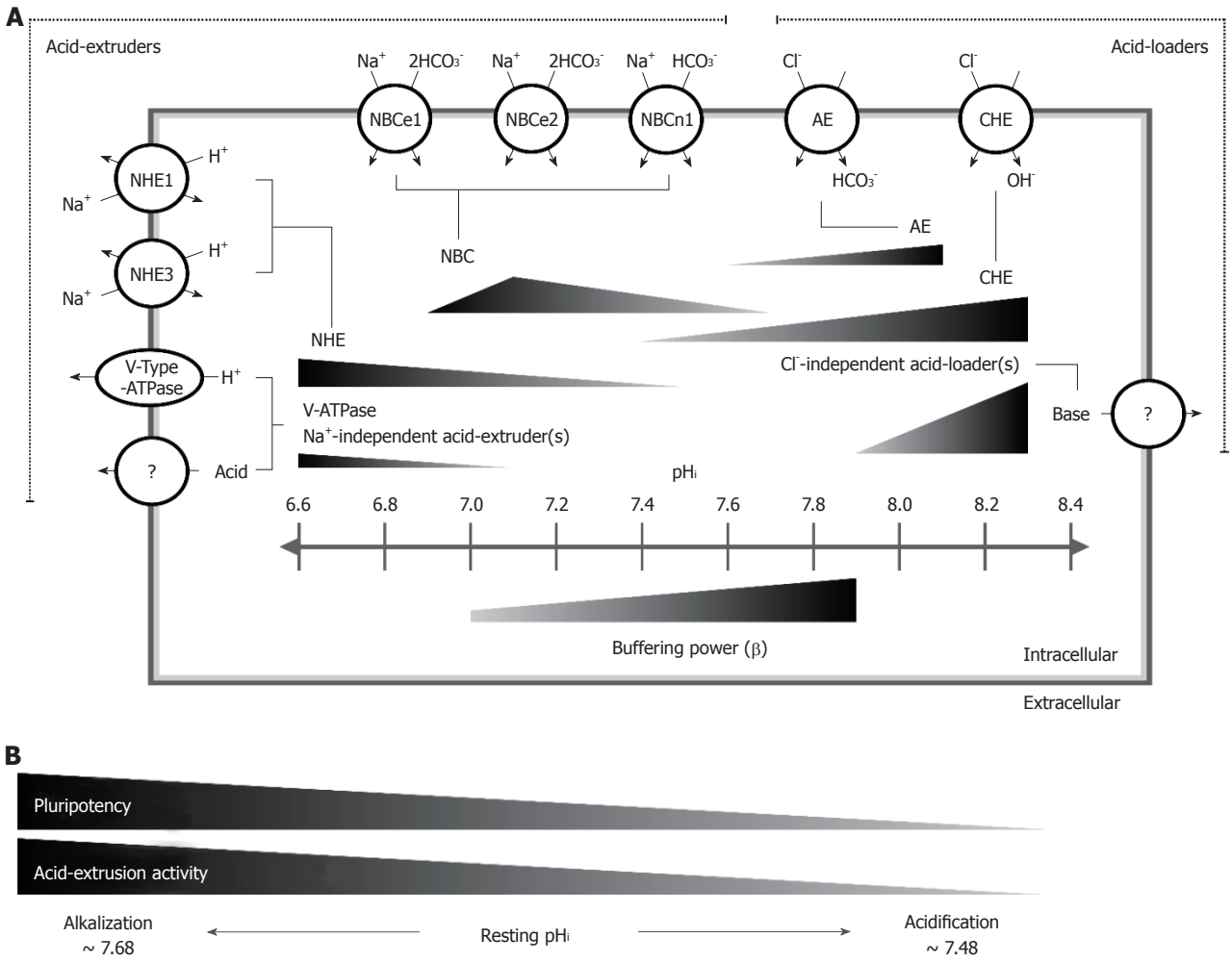


**Figure 7 Kinetic model of the pHi regulatory mechanism in human induced pluripotent stem cells.** A: A kinetic model illustrating the $pH_i$ regulatory mechanism in HPS0077 cell, including acid extrusion, acid loading and passive buffering power. For the first time, we demonstrated that the active membrane $pH_i$ regulators NHE1, NHE3, V-ATPase, NBCe1, NBCe2, NBCn1, AE and CHE functionally coexisted in hiPSCs, and in addition, unknown $Na^+$-independent acid extruder(s) and $Cl^-$-independent acid loader(s) were also observed. The length of the triangle indicates the $pH_i$ range of $pH_i$ regulator activation, and the height indicates the magnitude of the $pH_i$ regulatory activity. For example, the NHE, NBC, AE and CHE were activated at $pH_i \leqslant 7.5$, between 6.9 and 7.68, $\geqslant 7.4$ and between 7.6 and 8.1, respectively. The non-NHE acid extruders [V-ATPase, unknown $Na^+$-independent acid extruder(s)] and unknown $Cl^-$-independent acid loader(s) were activated during extreme intracellular acidification, *i.e.*, $pH_i < 7.1$, and alkalization, *i.e.*, $pH_i > 7.9$, respectively. Moreover, the intracellular passive buffering capacity (β) increased as the $pH_i$ shifted to the alkalization direction; B: In the process of the loss of pluripotency, the activity of the acid extrusion mechanism gradually decreased, including the participation of at least the NHE, the NBC and V-ATPase, and resulted in the resting $pH_i$ shifting from 7.68 to 7.48. hiPSCs: Human induced pluripotent stem cells; NHE: The $Na^+/H^+$ exchanger; NBC: The $Na^+/HCO_3^-$ cotransporter; V-ATPase: Vacuolar-ATPase; AE: Anion exchanger; CHE: $Cl^-$-$OH^-$ exchanger.

expression of pluripotency markers at a minimum $pH_e$ = 7.8[37,48,49]. The proliferative ability and pluripotency in hPSCs are critical for development[54]. Therefore, the expression of additional unknown $Na^-$-independent and $Cl^-$-independent acid-regulating extruder(s) in hiPSCs implicates the function of resisting the potential impact of intracellular proton changes in hPSCs. However, further study on characterizing the mechanisms should be conducted in the future.

### *Decreases in acid extrusion activity during the loss of pluripotency in hiPSCs*

A previous study showed that during the early spontaneous differentiation of mESCs, the resting $pH_i$ significantly increased at 48 and 72 h and returned to baseline at 96 h, and this increase was dependent on the loss of NHE1 function[6]. However, in this study, the decrease in resting $pH_i$ and the downregulation of the acid extrusion mechanism were demonstrated during the early loss of pluripotency in hiPSCs either in HEPES-buffered conditions or in 5% $CO_2/HCO_3^-$-buffered conditions. These contradictory results may be due to the different pluripotent states between mESCs and hiPSCs, *i.e.*, naïve and primed pluripotency, respectively[54,55]. As expected, the cells in the preprimed (naïve) and primed states significantly increased the $pH_i$ at 48 and 72 hours during early differentiation in mESCs. This result implies that increasing resting $pH_i$ occurred during the naïve to primed pluripotency states[6]. Subsequently, the resting $pH_i$ returned to baseline at 72-96 h, which may indicate that the primed state is further differentiated. Furthermore, to adapt to the intracellular acidification caused by increased glycolysis, *i.e.*, the Warburg effect, the acid extrusion

mechanism is upregulated and further alkalizes the resting $pH_i$ in cancer cells[24,26]. During the processes of PSC development, metabolism has been found to rely on different metabolic pathways, *i.e.*, oxidative phosphorylation (OXPHOS), glycolysis and OXPHOS in naive, primed and early differentiation states, respectively[51,56,57]. This switch between OXPHOS and glycolysis supports the dynamic changes in the resting $pH_i$ observed during the loss of pluripotency in mESCs and the decrease in the resting $pH_i$ and acid extrusion in hiPSCs demonstrated in this study.

The possible underlying mechanism for the observed decrease in the acid extrusion mechanism during the process of the loss of pluripotency in hiPSCs may be due to the crosstalk between the PI3K/AKT and MEK/ERK signaling pathways, which plays a curial role in pluripotency[58]. To maintain pluripotency in hPSCs, FGF2 has been added to the culture medium to activate PI3K/AKT signaling[58,59]. The activation of PI3K/AKT signaling further promotes the relative gene expression of pluripotency markers and inhibits differentiation by suppressing MEK/ERK signaling[58]. Therefore, the removal of FGF2 decreases the ratio of AKT activity to ERK and further causes cell differentiation[58,60]. ERK is a well-known activator of NHE1[61,62], but we did not find that removal of FGF2 (in E6 medium) resulted in an increase of the NHE1-dependent acid extrusion rate in this study. Although AKT has been shown to inhibit NHE1 activity in cardiovascular cells[63], AKT is stimulated by insulin and growth factors and further activates NHE1 in cancer cells and fibroblasts[64,65]. Therefore, this study implicates that the removal of FGF2 causes the loss of AKT activity and thus decreases the acid extrusion rate in hiPSCs.

In conclusion, for the first time, we established a functional $pH_i$ regulatory model in hiPSCs, as shown in Figure 7. In this model, we demonstrated that the steady-state $pH_i$ value is approximately 7.50-7.68 in hiPSCs. Additionally, we showed that at least four types of acid extruders [NHE, NBC, V-ATPase and $Na^+$-independent acid extruder(s)] and three types of acid loaders [CHE, AE and $Cl^-$-independent acid loader(s)] coexist and are responsible for the $pH_i$ regulatory mechanism, and each is activated in different $pH_i$ ranges in hiPSCs. Moreover, the activity of the acid extrusion mechanism decreased by changing both the expression and activity of acid extruders during the process of the loss of pluripotency in hiPSCs.

## ARTICLE HIGHLIGHTS

### Research background

Homeostasis of intracellular $pH_i$ ($pH_i$) affects many cellular functions, such as cell proliferation and differentiation. However, the knowledge of $pH_i$ regulation mechanism in human pluripotent stem cells still unknown.

### Research motivation

The changes of acid-base kinetic were observed during the loss of pluripotency in mouse embryonic stem cells. Moreover, the balance of intracellular and extracellular pH significantly affected the reprogramming efficiency and culture quality of human induced pluripotent stem cells (hiPSCs).

### Research objectives

We aimed to establish the $pH_i$ regulation mechanism model and investigate the relationship of $pH_i$ regulation and pluripotency in hiPSCs.

### Research methods

In the pluripotent state and during the loss of pluripotency in hiPSCs, we observed the activity of $pH_i$ regulation mechanism by acutely induced intracellular acidification and alkalization in the physiological buffered solution.

### Research results

In hiPSCs, the $Na^+$-$H^+$ exchanger (NHE), the $Na^+$-$HCO_3^-$ cotransporter (NBC) and vacuolar-ATPase (V-ATPase) were the main active acid extruders that were activated against intracellular acidification. In contrast, the acid-equivalent loaders, such as the $Cl^-$-$HCO_3^-$ anion exchanger (AE) and the $Cl^-$-$OH^-$ exchanger (CHE), were activated to prevent intracellular alkalization. In addition to the classic $pH_i$ regulators NHE, NBC, V-ATPase, AE and CHE, we also demonstrated the functional existence of unknown acid-extruder(s) and –loader(s) in hiPSCs. Moreover, the $pH_i$ and acid-extruding mechanism were decreased during the loss of pluripotency in hiPSCs.

### Research conclusions

For the first time, we established a model of the $pH_i$ regulation mechanism in hiPSCs. The higher resting $pH_i$ and acid-extruding mechanism might be the specific feature to adaptive the cancer-like cellular function and pluripotency in hiPSCs.

### Research perspectives

In summary, we characterized the $pH_i$ regulation mechanism and its functional/expressional roles in maintenance of pluripotency of hiPSCs. We proposed that targeting either $pH_i$ regulators or pH environments of culture medium could be an effective way to modify the pluripotency state of hiPSCs, which may contribute the differentiation efficiency or culture quality.

## REFERENCES


1 **Gao W**, Zhang H, Chang G, Xie Z, Wang H, Ma L, Han Z, Li Q, Pang T. Decreased intracellular pH induced by cariporide differentially contributes to human umbilical cord-derived mesenchymal stem cells differentiation. *Cell Physiol Biochem* 2014; **33**: 185-194 [PMID: 24481225 DOI: 10.1159/000356661]

2 **Li X**, Karki P, Lei L, Wang H, Fliegel L. Na+/H+ exchanger isoform 1 facilitates cardiomyocyte embryonic stem cell differentiation. *Am J Physiol Heart Circ Physiol* 2009; **296**: H159-H170 [PMID: 19011045 DOI: 10.1152/ajpheart.00375.2008]

3 **McBrian MA**, Behbahan IS, Ferrari R, Su T, Huang TW, Li K, Hong CS, Christofk HR, Vogelauer M, Seligson DB, Kurdistani SK. Histone acetylation regulates intracellular pH. *Mol Cell* 2013; **49**: 310-321 [PMID: 23201122 DOI: 10.1016/j.molcel.2012.10.025]

4 **Park HJ**, Lyons JC, Ohtsubo T, Song CW. Acidic environment causes apoptosis by increasing caspase activity. *Br J Cancer* 1999; **80**: 1892-1897 [PMID: 10471036 DOI: 10.1038/sj.bjc.6690617]

5 **Pouysségur J**, Franchi A, L'Allemain G, Paris S. Cytoplasmic pH, a key determinant of growth factor-induced DNA synthesis in quiescent fibroblasts. *FEBS Lett* 1985; **190**: 115-119 [PMID: 4043390 DOI: 10.1016/0014-5793(85)80439-7]

6 **Ulmschneider B**, Grillo-Hill BK, Benitez M, Azimova DR, Barber DL, Nystul TG. Increased intracellular pH is necessary for adult epithelial and embryonic stem cell differentiation. *J Cell Biol* 2016; **215**: 345-355 [PMID: 27821494 DOI: 10.1083/jcb.201606042]

7 **Loh SH**, Lee CY, Tsai YT, Shih SJ, Chen LW, Cheng TH, Chang CY, Tsai CS. Intracellular Acid-extruding regulators and the effect of lipopolysaccharide in cultured human renal artery smooth muscle cells. *PLoS One* 2014; **9**: e90273 [PMID: 24587308 DOI: 10.1371/journal.pone.0090273]

8 **Loh SH**, Chen WH, Chiang CH, Tsai CS, Lee GC, Jin JS, Cheng TH, Chen JJ. Intracellular pH regulatory mechanism in human atrial myocardium: functional evidence for Na(+)/H(+) exchanger and Na(+)/HCO(3)(-) symporter. *J Biomed Sci* 2002; **9**: 198-205 [PMID: 12065894 DOI: 10.1159/000059420]

9 **Loh SH**, Jin JS, Tsai CS, Chao CM, Chiung CS, Chen WH, Lin CI, Chuang CC, Wei J. Functional evidence for intracellular acid extruders in human ventricular myocardium. *Jpn J Physiol* 2002; **52**: 277-284 [PMID: 12230804 DOI: 10.2170/jjphysiol.52.277]

10 **Lagadic-Gossmann D**, Buckler KJ, Vaughan-Jones RD. Role of bicarbonate in pH recovery from intracellular acidosis in the guinea-pig ventricular myocyte. *J Physiol* 1992; **458**: 361-384 [PMID: 1302269 DOI: 10.1113/jphysiol.1992.sp019422]

11 **Amos BJ**, Pocock G, Richards CD. On the role of bicarbonate as a hydrogen ion buffer in rat CNS neurones. *Exp Physiol* 1996; **81**: 623-632 [PMID: 8853270 DOI: 10.1113/expphysiol.1996.sp003963]

12 **Chen GS**, Lee SP, Huang SF, Chao SC, Chang CY, Wu GJ, Li CH, Loh SH. Functional and molecular characterization of transmembrane intracellular pH regulators in human dental pulp stem cells. *Arch Oral Biol* 2018; **90**: 19-26 [PMID: 29524788 DOI: 10.1016/j.archoralbio.2018.02.018]

13 **Lee CY**, Tsai YT, Chang CY, Chang YY, Cheng TH, Tsai CS, Loh SH. Functional characterization of intracellular pH regulators responsible for acid extrusion in human radial artery smooth muscle cells. *Chin J Physiol* 2014; **57**: 238-248 [PMID: 25241983 DOI: 10.4077/CJP.2014.BAD269]

14 **Vaughan-Jones RD**, Spitzer KW, Swietach P. Intracellular pH regulation in heart. *J Mol Cell Cardiol* 2009; **46**: 318-331 [PMID: 19041875 DOI: 10.1016/j.yjmcc.2008.10.024]

15 **Casey JR**, Grinstein S, Orlowski J. Sensors and regulators of intracellular pH. *Nat Rev Mol Cell Biol* 2010; **11**: 50-61 [PMID: 19997129 DOI: 10.1038/nrm2820]

16 **de Hemptinne A**, Marrannes R, Vanheel B. Influence of organic acids on intracellular pH. *Am J Physiol* 1983; **245**: C178-C183 [PMID: 6614155 DOI: 10.1152/ajpcell.1983.245.3.C178]

17 **Trosper TL**, Philipson KD. Functional characteristics of the cardiac sarcolemmal monocarboxylate transporter. *J Membr Biol* 1989; **112**: 15-23 [PMID: 2593136 DOI: 10.1007/BF01871160]

18 **Deuticke B**, Beyer E, Forst B. Discrimination of three parallel pathways of lactate transport in the human erythrocyte membrane by inhibitors and kinetic properties. *Biochim Biophys Acta* 1982; **684**: 96-110 [PMID: 7055558 DOI: 10.1016/0005-2736(82)90053-0]

19 **Wang X**, Poole RC, Halestrap AP, Levi AJ. Characterization of the inhibition by stilbene disulphonates and phloretin of lactate and pyruvate transport into rat and guinea-pig cardiac myocytes suggests the presence of two kinetically distinct carriers in heart cells. *Biochem J* 1993; **290**(Pt 1): 249-258 [PMID: 8439293 DOI: 10.1042/bj2900249]

20 **Reshetnyak YK**. Imaging Tumor Acidity: pH-Low Insertion Peptide Probe for Optoacoustic Tomography. *Clin Cancer Res* 2015; **21**: 4502-4504 [PMID: 26224874 DOI: 10.1158/1078-0432.CCR-15-1502]

21 **Damaghi M**, Wojtkowiak JW, Gillies RJ. pH sensing and regulation in cancer. *Front Physiol* 2013; **4**: 370 [PMID: 24381558 DOI: 10.3389/fphys.2013.00370]

22 **Swietach P**, Vaughan-Jones RD, Harris AL, Hulikova A. The chemistry, physiology and pathology of pH in cancer. *Philos Trans R Soc Lond B Biol Sci* 2014; **369**: 20130099 [PMID: 24493747 DOI: 10.1098/rstb.2013.0099]

23 **Lee SP**, Chao SC, Huang SF, Chen YL, Tsai YT, Loh SH. Expressional and Functional Characterization of Intracellular pH Regulators and Effects of Ethanol in Human Oral Epidermoid Carcinoma Cells. *Cell Physiol Biochem* 2018; **47**: 2056-2068 [PMID: 29975935 DOI: 10.1159/000491473]

24 **Webb BA**, Chimenti M, Jacobson MP, Barber DL. Dysregulated pH: a perfect storm for cancer progression. *Nat Rev Cancer* 2011; **11**: 671-677 [PMID: 21833026 DOI: 10.1038/nrc3110]

25 **Hanahan D**, Weinberg RA. Hallmarks of cancer: the next generation. *Cell* 2011; **144**: 646-674 [PMID: 21376230 DOI: 10.1016/j.cell.2011.02.013]

26 **Parks SK**, Chiche J, Pouysségur J. Disrupting proton dynamics and energy metabolism for cancer therapy. *Nat Rev Cancer* 2013; **13**: 611-623 [PMID: 23969692 DOI: 10.1038/nrc3579]

27 **Moses C**, Garcia-Bloj B, Harvey AR, Blancafort P. Hallmarks of cancer: The CRISPR generation. *Eur J Cancer* 2018; **93**: 10-18 [PMID: 29433054 DOI: 10.1016/j.ejca.2018.01.002]

28 **Marchiq I**, Pouysségur J. Hypoxia, cancer metabolism and the therapeutic benefit of targeting lactate/H(+) symporters. *J Mol Med* (Berl) 2016; **94**: 155-171 [PMID: 26099350 DOI: 10.1007/s00109-015-1307-x]

29 **Lee ZW**, Teo XY, Song ZJ, Nin DS, Novera W, Choo BA, Dymock BW, Moore PK, Huang RY, Deng LW. Intracellular Hyper-Acidification Potentiated by Hydrogen Sulfide Mediates Invasive and Therapy Resistant Cancer Cell Death. *Front Pharmacol* 2017; **8**: 763 [PMID: 29163155 DOI: 10.3389/fphar.2017.00763]

30 **Amith SR**, Fliegel L. Regulation of the Na+/H+ Exchanger (NHE1) in Breast Cancer Metastasis. *Cancer Res* 2013; **73**: 1259-1264 [PMID: 23393197 DOI: 10.1158/0008-5472.CAN-12-4031]

31 **Lucien F**, Brochu-Gaudreau K, Arsenault D, Harper K, Dubois CM. Hypoxia-induced invadopodia formation involves activation of NHE-1 by the p90 ribosomal S6 kinase (p90RSK). *PLoS One* 2011; **6**: e28851 [PMID: 22216126 DOI: 10.1371/journal.pone.0028851]

32 **Takahashi K**, Tanabe K, Ohnuki M, Narita M, Ichisaka T, Tomoda K, Yamanaka S. Induction of pluripotent stem cells from adult human fibroblasts by defined factors. *Cell* 2007; **131**: 861-872 [PMID: 18035408 DOI: 10.1016/j.cell.2007.11.019]

33 **Gu W**, Gaeta X, Sahakyan A, Chan AB, Hong CS, Kim R, Braas D, Plath K, Lowry WE, Christofk HR. Glycolytic Metabolism Plays a Functional Role in Regulating Human Pluripotent Stem Cell State. *Cell Stem Cell* 2016; **19**: 476-490 [PMID: 27618217 DOI: 10.1016/j.stem.2016.08.008]

34 **Yoshida Y**, Takahashi K, Okita K, Ichisaka T, Yamanaka S. Hypoxia enhances the generation of induced pluripotent stem cells. *Cell Stem Cell* 2009; **5**: 237-241 [PMID: 19716359 DOI: 10.1016/j.stem.2009.08.001]

35 **Zhang J**, Nuebel E, Daley GQ, Koehler CM, Teitell MA. Metabolic regulation in pluripotent stem cells during reprogramming and self-renewal. *Cell Stem Cell* 2012; **11**: 589-595 [PMID: 23122286 DOI: 10.1016/j.stem.2012.10.005]

36 **Wang H**, Singh D, Fliegel L. The Na+/H+ antiporter potentiates growth and retinoic acid-induced differentiation of P19 embryonal carcinoma cells. *J Biol Chem* 1997; **272**: 26545-26549 [PMID: 9334233 DOI: 10.1074/jbc.272.42.26545]

37 **Chaudhry MA**, Bowen BD, Piret JM. Culture ph and osmolality influence proliferation and embryoid body yields of murine embryonic stem cells. *Biochem Eng J* 2009; **45**: 126-135 [DOI: 10.1016/j.bej.2009.03.005]

38 **Zaniboni M**, Swietach P, Rossini A, Yamamoto T, Spitzer KW, Vaughan-Jones RD. Intracellular proton mobility and buffering power in cardiac ventricular myocytes from rat, rabbit, and guinea pig. *Am J Physiol Heart Circ Physiol* 2003; **285**: H1236-H1246 [PMID: 12750065 DOI: 10.1152/ajpheart.00277.2003]

39 **Leem CH**, Lagadic-Gossmann D, Vaughan-Jones RD. Characterization of intracellular pH regulation in the guinea-pig ventricular myocyte. *J Physiol* 1999; **517** ( Pt 1): 159-180 [PMID: 10226157 DOI: 10.1111/j.1469-7793.1999.0159z.x]

40 **Boedtkjer E**, Aalkjaer C. Acid-base transporters modulate cell migration, growth and proliferation: Implications for structure development and remodeling of resistance arteries? *Trends Cardiovasc Med* 2013; **23**: 59-65 [PMID: 23266155 DOI: 10.1016/j.tcm.2012.09.001]

41 **Romero MF**, Chen AP, Parker MD, Boron WF. The SLC4 family of bicarbonate ($HCO_3^-$) transporters. *Mol Aspects Med* 2013; **34**: 159-182 [PMID: 23506864 DOI: 10.1016/j.mam.2012.10.008]

42 **Boedtkjer E**, Aalkjaer C. Intracellular pH in the resistance vasculature: regulation and functional implications. *J Vasc Res* 2012; **49**: 479-496 [PMID: 22907294 DOI: 10.1159/000341235]

43 **da Costa-Pessoa JM**, Damasceno RS, Machado UF, Beloto-

Silva O, Oliveira-Souza M. High glucose concentration stimulates NHE-1 activity in distal nephron cells: the role of the Mek/Erk1/2/p90RSK and p38MAPK signaling pathways. *Cell Physiol Biochem* 2014; **33**: 333-343 [PMID: 24557342 DOI: 10.1159/000356673]

44 **Li X**, Wang T, Zhao Z, Weinman SA. The ClC-3 chloride channel promotes acidification of lysosomes in CHO-K1 and Huh-7 cells. *Am J Physiol Cell Physiol* 2002; **282**: C1483-C1491 [PMID: 11997263 DOI: 10.1152/ajpcell.00504.2001]

45 **Takahashi Y**, Fujii T, Fujita K, Shimizu T, Higuchi T, Tabuchi Y, Sakamoto H, Naito I, Manabe K, Uchida S, Sasaki S, Ikari A, Tsukada K, Sakai H. Functional coupling of chloride-proton exchanger ClC-5 to gastric H+,K+-ATPase. *Biol Open* 2014; **3**: 12-21 [PMID: 24429108 DOI: 10.1242/bio.20136205]

46 **Dascalu A**, Nevo Z, Korenstein R. The control of intracellular pH in cultured avian chondrocytes. *J Physiol* 1993; **461**: 583-599 [PMID: 8394427 DOI: 10.1113/jphysiol.1993.sp019530]

47 **Theparambil SM**, Naoshin Z, Thyssen A, Deitmer JW. Reversed electrogenic sodium bicarbonate cotransporter 1 is the major acid loader during recovery from cytosolic alkalosis in mouse cortical astrocytes. *J Physiol* 2015; **593**: 3533-3547 [PMID: 25990710 DOI: 10.1113/JP270086]

48 **Kim N**, Minami N, Yamada M, Imai H. Immobilized pH in culture reveals an optimal condition for somatic cell reprogramming and differentiation of pluripotent stem cells. *Reprod Med Biol* 2016; **16**: 58-66 [PMID: 29259452 DOI: 10.1002/rmb2.12011]

49 **Gupta P**, Hourigan K, Jadhav S, Bellare J, Verma P. Effect of lactate and ph on mouse pluripotent stem cells: Importance of media analysis. *Biochem Eng J* 2017; **118**: 25-33 [DOI: 10.1016/j.bej.2016.11.005]

50 **Liu A**, Yu X, Liu S. Pluripotency transcription factors and cancer stem cells: small genes make a big difference. *Chin J Cancer* 2013; **32**: 483-487 [PMID: 23419197 DOI: 10.5732/cjc.012.10282]

51 **Varum S**, Rodrigues AS, Moura MB, Momcilovic O, Easley CA 4th, Ramalho-Santos J, Van Houten B, Schatten G. Energy metabolism in human pluripotent stem cells and their differentiated counterparts. *PLoS One* 2011; **6**: e20914 [PMID: 21698063 DOI: 10.1371/journal.pone.0020914]

52 **Tsai CS**, Loh SH, Jin JS, Hong GJ, Lin HT, Chiung CS, Chang CY. Effects of alcohol on intracellular pH regulators and electromechanical parameters in human myocardium. *Alcohol Clin Exp Res* 2005; **29**: 1787-1795 [PMID: 16269908 DOI: 10.1097/01.alc.0000183512.31705.74]

53 **Tsai YT**, Lee CY, Hsu CC, Chang CY, Hsueh MK, Huang EY, Tsai CS, Loh SH. Effects of urotensin II on intracellular pH regulation in cultured human internal mammary artery smooth muscle cells. *Peptides* 2014; **56**: 173-182 [PMID: 24768794 DOI: 10.1016/j.peptides.2014.04.011]

54 **Weinberger L**, Ayyash M, Novershtern N, Hanna JH. Dynamic stem cell states: naive to primed pluripotency in rodents and humans. *Nat Rev Mol Cell Biol* 2016; **17**: 155-169 [PMID: 26860365 DOI: 10.1038/nrm.2015.28]

55 **Altshuler A**, Verbuk M, Bhattacharya S, Abramovich I, Haklai R, Hanna JH, Kloog Y, Gottlieb E, Shalom-Feuerstein R. RAS Regulates the Transition from Naive to Primed Pluripotent Stem Cells. *Stem Cell Reports* 2018; **10**: 1088-1101 [PMID: 29456180 DOI: 10.1016/j.stemcr.2018.01.004]

56 **Folmes CD**, Dzeja PP, Nelson TJ, Terzic A. Metabolic plasticity in stem cell homeostasis and differentiation. *Cell Stem Cell* 2012; **11**: 596-606 [PMID: 23122287 DOI: 10.1016/j.stem.2012.10.002]

57 **Ryall JG**, Cliff T, Dalton S, Sartorelli V. Metabolic Reprogramming of Stem Cell Epigenetics. *Cell Stem Cell* 2015; **17**: 651-662 [PMID: 26637942 DOI: 10.1016/j.stem.2015.11.012]

58 **Singh AM**, Reynolds D, Cliff T, Ohtsuka S, Mattheyses AL, Sun Y, Menendez L, Kulik M, Dalton S. Signaling network crosstalk in human pluripotent cells: a Smad2/3-regulated switch that controls the balance between self-renewal and differentiation. *Cell Stem Cell* 2012; **10**: 312-326 [PMID: 22385658 DOI: 10.1016/j.stem.2012.01.014]

59 **Chen G**, Gulbranson DR, Hou Z, Bolin JM, Ruotti V, Probasco MD, Smuga-Otto K, Howden SE, Diol NR, Propson NE, Wagner R, Lee GO, Antosiewicz-Bourget J, Teng JM, Thomson JA. Chemically defined conditions for human iPSC derivation and culture. *Nat Methods* 2011; **8**: 424-429 [PMID: 21478862 DOI: 10.1038/nmeth.1593]

60 **Cho YM**, Kwon S, Pak YK, Seol HW, Choi YM, Park DJ, Park KS, Lee HK. Dynamic changes in mitochondrial biogenesis and antioxidant enzymes during the spontaneous differentiation of human embryonic stem cells. *Biochem Biophys Res Commun* 2006; **348**: 1472-1478 [PMID: 16920071 DOI: 10.1016/j.bbrc.2006.08.020]

61 **Malo ME**, Li L, Fliegel L. Mitogen-activated protein kinase-dependent activation of the Na+/H+ exchanger is mediated through phosphorylation of amino acids Ser770 and Ser771. *J Biol Chem* 2007; **282**: 6292-6299 [PMID: 17209041 DOI: 10.1074/jbc.M611073200]

62 **Javadov S**, Baetz D, Rajapurohitam V, Zeidan A, Kirshenbaum LA, Karmazyn M. Antihypertrophic effect of Na+/H+ exchanger isoform 1 inhibition is mediated by reduced mitogen-activated protein kinase activation secondary to improved mitochondrial integrity and decreased generation of mitochondrial-derived reactive oxygen species. *J Pharmacol Exp Ther* 2006; **317**: 1036-1043 [PMID: 16513848 DOI: 10.1124/jpet.105.100107]

63 **Snabaitis AK**, Cuello F, Avkiran M. Protein kinase B/Akt phosphorylates and inhibits the cardiac Na+/H+ exchanger NHE1. *Circ Res* 2008; **103**: 881-890 [PMID: 18757828 DOI: 10.1161/CIRCRESAHA.108.175877]

64 **Meima ME**, Webb BA, Witkowska HE, Barber DL. The sodium-hydrogen exchanger NHE1 is an Akt substrate necessary for actin filament reorganization by growth factors. *J Biol Chem* 2009; **284**: 26666-26675 [PMID: 19622752 DOI: 10.1074/jbc.M109.019448]

65 **Clement DL**, Mally S, Stock C, Lethan M, Satir P, Schwab A, Pedersen SF, Christensen ST. PDGFRα signaling in the primary cilium regulates NHE1-dependent fibroblast migration via coordinated differential activity of MEK1/2-ERK1/2-p90RSK and AKT signaling pathways. *J Cell Sci* 2013; **126**: 953-965 [PMID: 23264740 DOI: 10.1242/jcs.116426]

**P- Reviewer**: Saeki K, Tanabe S **S- Editor**: Ma YJ
**L- Editor**: A **E- Editor**: Song H

Published by **Baishideng Publishing Group Inc**
7901 Stoneridge Drive, Suite 501, Pleasanton, CA 94588, USA
Telephone: +1-925-223-8242
Fax: +1-925-223-8243
E-mail: bpgoffice@wjgnet.com
Help Desk: https://www.f6publishing.com/helpdesk
https://www.wjgnet.com